Untapped Potential of Moorochloa eruciformis (Sm.) Veldkamp: Metabolomic Insights into its Antioxidant and in vitro Enzyme-Inhibiting Properties

Alia Y. Ragheb
National Research Centre
Mona El Shabrawy
mona.elshabrawy75@gmail.com
National Research Centre
Amal G. Hussien
National Research Centre
Mona E. S. Kassem
National Research Centre
Mona M. Marzouk
National Research Centre

Article

Keywords: Acetylcholinesterase, Brachiaria eruciformis, Flavonolignans, Hydroxybenzoic acid derivatives, Molecular networking, Weeds

Posted Date: November 19th, 2025

DOI: https://doi.org/10.21203/rs.3.rs-7790634/v1

Additional Declarations: No competing interests reported.

Untapped Potential of *Moorochloa eruciformis* (Sm.) Veldkamp: Metabolomic Insights into its Antioxidant and *in vitro* Enzyme-Inhibiting Properties

Alia Y. Ragheb [1, 2], Mona El Shabrawy [1*], Amal G. Hussien [3], Mona E. S. Kassem [1], Mona M. Marzouk [1]

[1] Phytochemistry and Plant Systematics Department, Pharmaceutical and Drug Industries Research Institute, National Research Centre, 33 El Bohouth St. (Former El Tahrir St.), Dokki, Giza, 12622, Egypt.

[2] Pharmacognosy Department, Faculty of Pharmacy, Sadat City University, Sadat City, 32897, Egypt.

[3] Biochemistry Department, Biotechnology Research Institute, National Research Centre, 33 El Bohouth St. (Former El Tahrir St.), Dokki, Giza, 12622, Egypt.

*Correspondence: mona.elshabrawy75@gmail.com

Abstract

Although unintentionally grown weeds are often seen as a problematic issue because they may compete with desired plants for resources, they can also possess positive and beneficial qualities. In many Poaceae crops, *Moorochloa eruciformis* (Sm.) Veldkamp is an invasive weed and is often discarded, wasting its potential. To utilize the *M. eruciformis*, extracts from petroleum ether, 70% aqueous methanol, and defatted aqueous methanol were screened *in vitro* for their ability to scavenge radicals and inhibit certain diagnostic enzymes. The defatted aqueous methanol exhibited the most significant antioxidant, anti-Alzheimer, and antidiabetic attributes as well as moderate anti-inflammatory effect. Additionally, the same extract was found to contain the major phenolic content as determined spectrophotometrically. Therefore, it was further characterized through LC-ESI-MS in conjunction with GNPS-based molecular networking, aiming to discover the metabolic profile responsible for these impacts. As a result, 102 metabolites were annotated for the first time for the species, encompassing unique derivatives of hydroxycinnamic and hydroxybenzoic acids

as well as flavonolignans. *M. eruciformis* could be recycled and validated as a valuable source of natural phenolic acids and flavonoids, supporting its consideration in clinical research on natural antioxidant and anti-inflammatory agents for arthritis, diabetes, and Alzheimer's diseases.

Keywords

Acetylcholinesterase, *Brachiaria eruciformis*, Flavonolignans, Hydroxybenzoic acid derivatives, Molecular networking, Weeds

1. Introduction

The *Poaceae* family (also known as *Gramineae*, the grass family) is undisputedly the most economically and ecologically important plant family to humanity; it comprises approximately 12000 species and over 800 accepted genera [1]. It is the main source of the world's most important staple crops, "cereal", such as wheat, rice, barley, oats, and maize, the primary source of sugar, like sugarcane, and an essential source of livestock forage, such as sorghum, where many species are cultivated as pasture and fodder [2].

Besides, in agricultural fields, grass is a significant source of weeds, as many of the most problematic weeds in cultivated fields are grasses. They are considered invasive plants that persist in infesting agricultural lands, demonstrating their ability to colonize, transform environments, and compete for resources like light, water, space, soil moisture, and nutrients [3], thereby affecting the yield of food and fiber crops. Despite their negative reputation, when properly managed, they offer several advantages to agricultural ecosystems and crop yield [4]. They can provide food sources and habitats for beneficial insects such as pollinators. Additionally, their deep root systems help improve water infiltration and aeration, and some have the ability to transport nutrients from deeper soil layers to the surface, which helps enhance soil fertility [5].

On the other hand, many plants of the family are used as anti-inflammatory, anticancer antidiabetic, antimicrobial, and antioxidant agents [1]. Additional pharmacological potential antihypertensives [6], anthelmintics [7], antiulcer [8], and diuretics [9]. Their uses are attributed to phenolic compounds, saponins, essential oils, coumarins, terpenoids, vitamins, glycosides, and alkaloids [1], flavonoids and carotenoids [10], which were reported in this family.

*Moorochloa eruciformis (*Sm.) Veldkamp, known as "sweet signal grass" or "sweet summer grass," was formerly classified as *Brachiaria eruciformis* (J.E. Sm.) Griseb. but has recently been reclassified into the genus *Moorochloa* based on distinct features of the fertile floret. It has also been recognized as *Panicum eruciforme* J.E. Smith and *Panicum wightii* Nees. This annual weed is regarded as a noxious weed of cultivation in many regions, especially in unirrigated systems. It is primarily used as forage or fodder in various native areas of Africa, the Mediterranean Region, and much of Asia [11]. Limited information exists on other uses because research on its benefits is scarce. In Egypt, Boulos [12] documented its presence as a weed of cultivation throughout the Nile region, the Egyptian Oases, and the Sinai Peninsula. However, it mainly acts as a competitive weed in Egyptian rice fields. This aligns with its known traits as a fast-growing plant with high seed production capacity that can form a dense grass mat in cropped fields, likely leading to interference and significant yield loss in the sorghum and cotton-growing areas [13].

Many reports revealed the presence of high phenolic contents in *Moorochloa* and *Brachiaria* grasses; others reported the presence of terpenoids, steroid saponins, large amounts of flavonoids, tannins, and alkaloids that could be beneficial to the growth and productivity of animals consuming them [14].

Considering *M. eruciformis* weed as just a plant growing in the wrong place, belonging to the same Poaceae family, suggests that it has similar important biological impacts. In addition,

there has been no phytochemical screening to identify its potential medicinal properties, and its biological activities have not been extensively researched. The presence of these chemical compounds in other *Moorochloa* (= *Brachiaria*) species makes it a promising candidate for future research for this lesser-known plant.

To understand how we can benefit from this wasted weed plant, our study investigated the antioxidant, antidiabetic, anti-Alzheimer, and anti-arthritic potential of *M. eruciformis* leaves. Three extracts were prepared: petroleum ether (PEE), 70% aqueous methanol (AME), and defatted aqueous methanol (DAME), and their *in vitro* inhibitory activity was assessed against the key enzymes *α*-amylase, *α*-glucosidase, acetylcholinesterase (AchE), and proteinase. In addition, the phenolic and condensed tannin contents were quantified. As a result, the metabolome profile of the most effective extract that contained abundant phytochemicals responsible for these activities (aqueous methanol leaves extract) was explored through a comprehensive HPLC MS/MS integrated with GNPS molecular networking as we could potentially find new uses for this plant in areas such as natural pharmaceuticals or other valuable bioproducts instead of focusing solely on eradication, thereby benefiting the agricultural ecosystem and human industry.

2. Materials and Methods

2.1. Plant material: collection, preparation, and extraction

M. eruciformis whole plant was collected by Mona E. S. Kassem (Co-author) with ethics requirements (Approval number: 20218) from Shubra Wasim, El-Beheira, Egypt, on 23 September 2020, https://maps.app.goo.gl/2muWZc7xAt3Gz23t8?g_st=iw, and identified according to Boulos (2005) by Dr Mona M. Marzouk (Co-author). A voucher specimen (No. M2065) was placed in CAIRC (the herbarium of National Research Centre).

The collected individuals were washed with tap water to remove the particulates and dust. Washed individuals were stored between two filter paper sheets to remove excess water, then left in the shade at room temperature till totally dry. The dried ground powder was soaked in methanol (70%) at room temperature overnight (several times, till exhausted), then filtered to remove any residual powder. A rotary evaporator (Heidolph) was used to evaporate the solvent at 70°C until dryness, yielding a brown residue regarding the total aqueous methanol extract (AME). Furthermore, AME was defatted by petroleum ether (60-80° C), yielding the petroleum ether extract (PEE) and defatted aqueous methanol extract (DAME) [15]. Part of each extract was used for the assessment of antioxidant, antidiabetic, anti-Alzheimer, and anti-arthritic activities [16].

2.2. Biological investigation

2.2.1. Antioxidant and radical scavenging evaluation

For AME, PEE, and DAME, total antioxidant capacity (TAC) was measured as mg gallic acid equivalent per gram dry weight, while total iron-reducing power (TIRP) was assayed as µg/mL followed the method by Farid et al. [16]. Moreover, the scavenging activities of the extract were assayed against DPPH (1,1-Diphenyl-2-picryl-hydrazyl) and ABTS (2,2'-azinobis-(3-ethylbenzothiazoline-6-sulfonic acid) radicals. The median inhibitory concentration (IC_{50}) against DPPH• and the percentage of inhibitory effect against ABTS• were determined using ascorbic acid as a standard according to the described method [16].

2.2.2. In Vitro Enzymes Inhibitory Assessment: Antidiabetic, anti-Alzheimer, and anti-arthritic evaluation

The anti-diabetic activities of AME, PEE, and DAME were determined by assessing the % inhibition of α-amylase and α-glucosidase enzymes according to the reported methods using acarbose as a positive control [17].

Moreover, the anti-Alzheimer's assessment for the three extracts was determined by determining the (%) inhibition of the acetylcholinesterase enzyme (AChE) using donepezil as a standard drug according to Farid et al [16].

Finally, anti-arthritic properties were evaluated by determining the % inhibition of protein denaturation and proteinase enzymes. To measure the % inhibition of protein denaturation, a standard non-steroidal anti-inflammatory drug (NSAID), diclofenac sodium, was used for comparison. The process involved preparing two main solution types. First, a test control was made by combining bovine serum albumin (BSA) (0.45 mL), a protein, with distilled water (0.05 mL). Second, a product control (0.5 mL) was prepared for each sample concentration by mixing a small amount of the sample (0.05 mL) with distilled water (0.45 mL). After adjusting the pH of all solutions to 6.3 with hydrochloric acid (1N), the samples were subjected to a two-step heating process: 20 minutes at 37°C, followed by 3 minutes at 57°C. Following the heating and a subsequent cooling period, a phosphate buffer (2.5 mL) was added. The final step was to measure the absorbance of each solution at 416 nm using a UV-Visible spectrophotometer, which allowed for the calculation of the percentage of protein denaturation inhibition.

The % inhibition of the proteinase enzyme was measured by combining each sample (1 mL), at each concentration, with a reaction mixture containing trypsin (0.06 mg) in Tris HCl buffer (1 mL of 20 mM). This mixture was then incubated at 37°C for 5 minutes, after which 1 mL of casein (0.8% w/v) was added. After a further 20-minute incubation, 2 mL of perchloric acid (70%) was

added to stop the reaction. The cloudy suspension was then centrifuged, and the absorbance of the supernatant was measured at 210 nm against the buffer as the blank [18].

2.2.3. Statistical analysis

All measurements were obtained from three replicates (n=3) and presented as mean ± standard error (SE). A one-way ANOVA was conducted using the Statistical Package for the Social Sciences (SPSS for Windows®, Version 11.0, 2001, SPSS Inc., Chicago, USA), followed by the Bonferroni post-hoc test to evaluate statistically significant differences among the various measurements. A p-value of ≤ 0.05 was considered indicative of statistical significance [18].

2.3. Phytochemical investigation

2.3.1. Total phenol contents

The concentration of total phenol content was quantified as mg gallic acid/100 g according to Aboulthana et al. [19].

2.3.2. LC-ESI-MS/MS and molecular networking analysis of DAME

The LC-ESI-MS/MS measurement of DAME was performed on Exion LC AC system coupled with a SCIEX Triple Quad 5500+ MS/MS platform, following the procedure illustrated by Marthouk et al. [17]. The MS data was processed using PeakView® Software 1.2. A negative-mode molecular network was generated using the GNPS platform (http://gnps.ucsd.edu) on August 7, 2024, in which the raw data file of DAME was converted into the open-format (.mzML) via the MSConvert package and subsequently uploaded to GNPS through WinSCP. The precursor ion mass tolerance and a MS/MS fragment ion tolerance were set to 2.0 Da and 0.5 Da, respectively.

158 A negative network was then created where edges were filtered to have a cosine score
159 above 0.7 and more than 6 matched peaks. Further, the maximum size of a molecular family was
160 set to 50. The spectra in the network were then searched against GNPS' spectral libraries. All
161 matches kept between network spectra and library spectra were required to have a score above 0.7
162 and at least 6 matched peaks [20]. Finally, the molecular network was further visualized by
163 Cytoscape 3.8.2.
164
165 **3. Results and discussion**
166 **3.1. Biological investigation**
167 *3.1.1. Antioxidant and radical scavenging evaluation*
168 Among the tested extracts, DAME displayed the best antioxidant and scavenging
169 capabilities, including total antioxidant capacity (211.31 ± 1.26 mg gallic acid/gm), iron-reducing
170 power (123.27 ± 0.74 µg/mL), and ABTS scavenging activity (50.31 %). In addition, the lowest
171 IC_{50} value of DAME (4.73 ± 0.30 µg/ml) that could approach the efficacy of ascorbic acid (3.94 ±
172 0.03 µg/ml) suggested its powerful effect, which may correlate to its rich phytochemical profile.
173 Conversely, PEE exhibited the weakest antioxidant results (**Figure 1**).
174

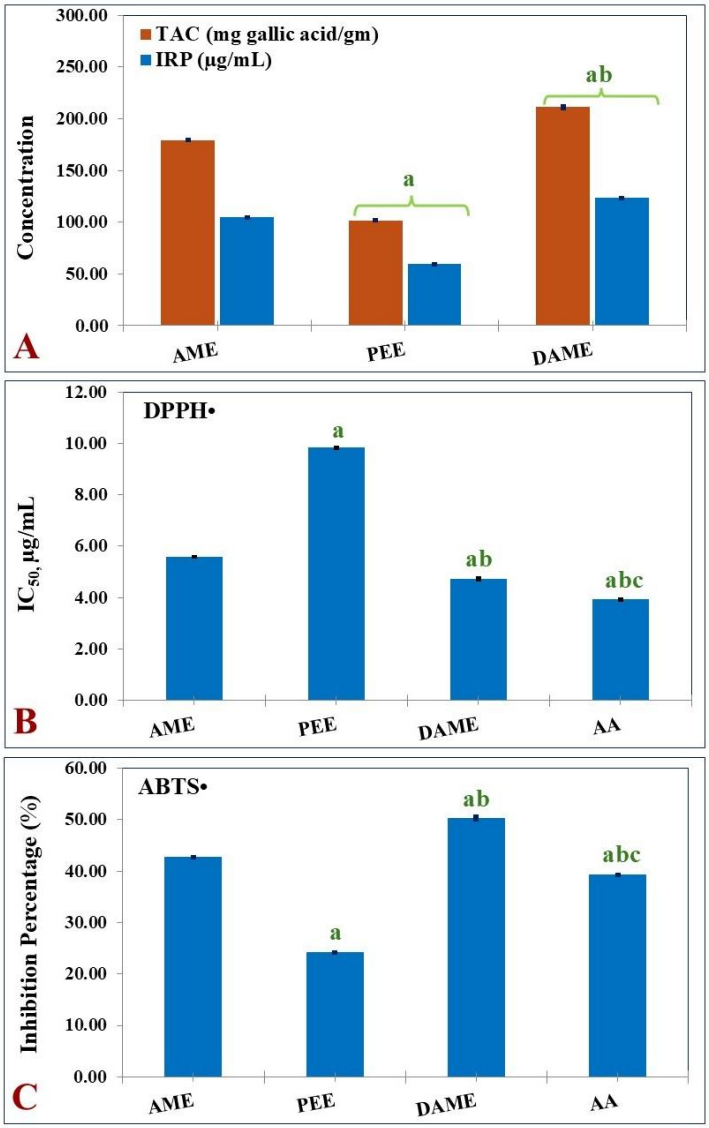

Figure 1: The *in vitro* antioxidant and radical scavenging evaluation of different *M. eruciformis* whole plant extracts: AME (70% aqueous methanol extract), PEE (petroleum ether extract), DAME (defatted aqueous methanol extract) against **A**; total antioxidant capacity (TAC) and iron-reducing power (IRP) **B**; 1,1-Diphenyl-2-picryl-hydrazyl (DPPH) and **C**; 2,2'-azinobis-(3-ethylbenzothiazoline-6-sulfonic acid) (ABTS) radical using ascorbic acid (AA) standard. Values were expressed as mean ± SE (calculated from three replicates). **a**: denotes the statistical difference from AME, **b**: denotes the statistical difference from PEE, and **c**: denotes the statistical difference from DAME at $p \leq 0.05$.

3.1.2. Antidiabetic, anti-Alzheimer, and anti-arthritic evaluation

Regarding the antidiabetic activity, DAME showed the most significant inhibitory effect against α-amylase (30.19 ± 0.18 %) and α-glucosidase (21.19 ± 0.18 %) enzymes, but still lower

than their respective acarbose standard effect (67.2 ± 0.02 and 53.31 ± 0.01 %, respectively). Likewise, the acetylcholinesterase (AChE) inhibitory activity of the same extract was higher (39.86 ± 0.09 %) than AME and PEE, and lower than the donepezil standard (69 ± 0.04%). For the anti-arthritic activity, the three extracts showed similar and moderate inhibition percentages of proteinase enzyme and proteinase denaturation to diclofenac sodium (**Figure 2**).

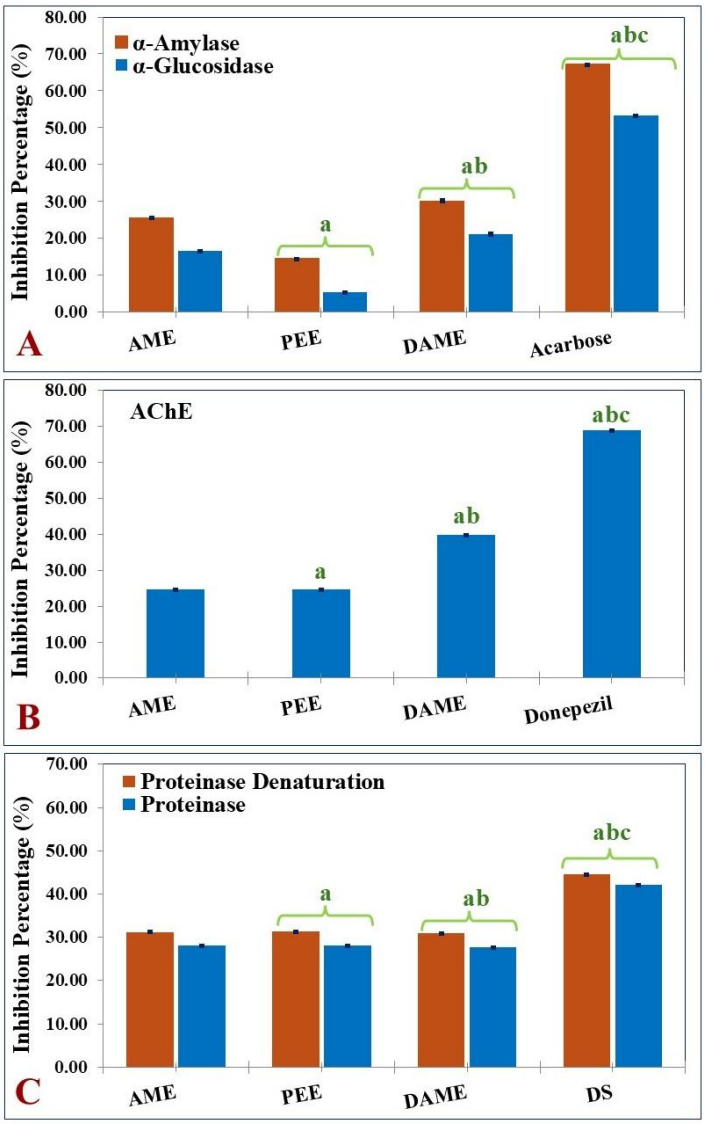

Figure 2: The *in vitro* biological evaluation of different *M. eruciformis* whole plant extracts: AME (70% aqueous methanol extract), PEE (petroleum ether extract), DAME (defatted aqueous methanol extract) **A;** anti-diabetic activity against acarbose, **B**; anti-Alzheimer activity against donepezil, and **C**; anti-arthritic activity against diclofenac sodium (DS). Values were expressed as mean ± SE (calculated from three replicates). **a**: denotes the statistical difference from AME, **b**: denotes the statistical difference from PEE, and **c**: denotes the statistical difference from DAME at $p \leq 0.05$.

205
206 **3.2. Phytochemical investigation**

207 Polarity-guided extraction was performed to simplify the complicated species extract by
208 separating the compounds with similar chemical properties, often concentrating their bioactivity,
209 yielding three distinct extracts (PEE, AME, and DAME). Screening for relevant *in vitro*
210 bioactivities, DAME demonstrated considerably higher inhibitory impacts and a significantly
211 lower IC_{50} value across antioxidant, anti-Alzheimer, and antidiabetic assays compared to PEE and
212 AME. Consequently, DAME was selected for detailed metabolome profiling, starting with the
213 estimation of phenolic and condensed tannin contents, followed by liquid chromatography-
214 electrospray ionization-mass spectrometry (LC-ESI-MS/MS) combined with Global Natural
215 Products Social (GNPS) molecular networking (MN). This bioactivity-guided metabolomics
216 approach allows for the identification of multiple active compounds, aims to avoid replication of
217 known metabolites, and utilizes networking to cluster unknown compounds with known bioactive,
218 making them valuable targets for drug discovery.

219 **3.2.1. Total phenolic contents**

220 DAME of *M. eruciformis* demonstrated the highest phenolic content (88.05 ± 0.53 mg
221 gallic acid/100 gm) compared to those of AME (74.78 ± 0.02 mg gallic acid/100 gm) and PEE
222 (42.39 ± 0.08 mg gallic acid/100 gm).

223 **3.2.2. Molecular networking aided LC-ESI-MS/MS**

224 The detailed chemical profile of DMAE from *M. eruciformis* was analysed using LC-ESI-
225 MS/MS in negative ionization mode to generate a base peak chromatogram (**Figure 3**), which
226 highlights the diversity and relative abundance of compound classes. The data were processed with
227 the GNPS molecular networking platform, grouping similar molecules based on their mass spectra.
228 These relationships are organized and visualized as a network to better illustrate the complexity of

the species. The molecular network was constructed from 315 nodes forming 35 clusters of 154 connected components with similar fragmentation patterns (at least two-node connected cluster) and 161 self-looped nodes. Notable clusters **A**, **B**, **C**, **D**, **E**, **F**, **G**, **H**, **I**, **J**, and **K** (**Figure 4**) guided the identification of several phenolic classes and many phospholipids. Their characterization was confirmed by analyzing their molecular ions, fragmentation peaks with intensities, retention times, GNPS spectral similarities, and comparing these fragmentation data with previous studies (Table 1).

In total, 102 metabolites were identified, including the crucial effective metabolites that could serve as a source of most derived plant medicine, which were 11 phospholipids and 83 phenolic compounds (39 phenolic acids and their derivatives and 44 flavonoids) (**Table 1**). Those compounds are valued for their potential health benefits, particularly their antioxidant properties. On the other hand, some organic acids, amino acids, and saccharides were also characterized.

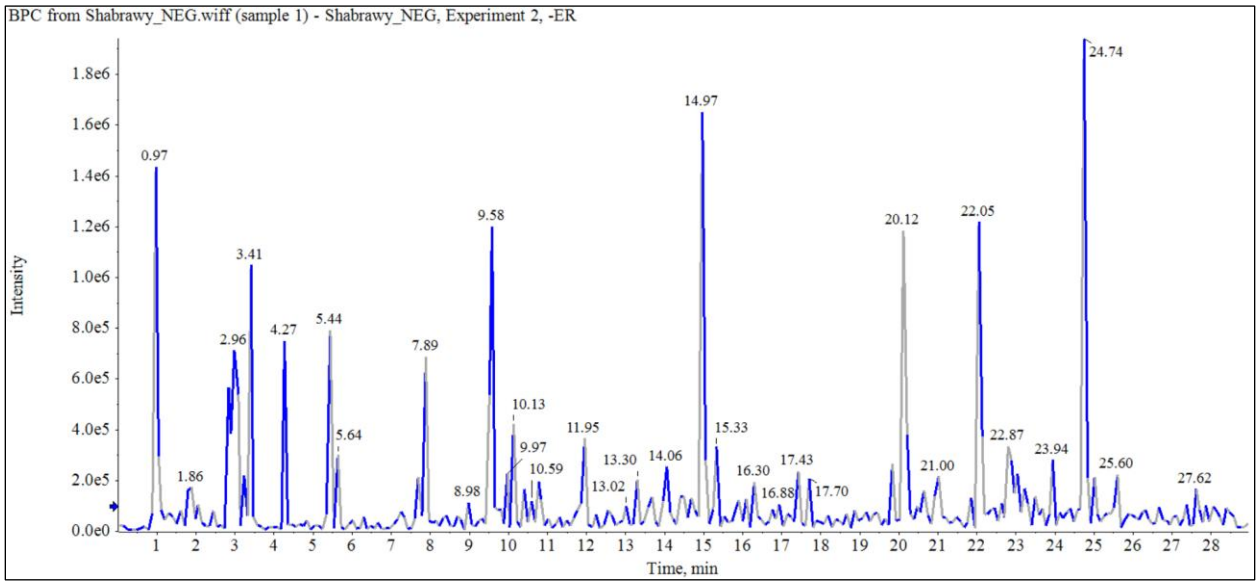

Figure 3. The base peak chromatogram of the defatted aqueous extract of *M. eruciformis* whole plant

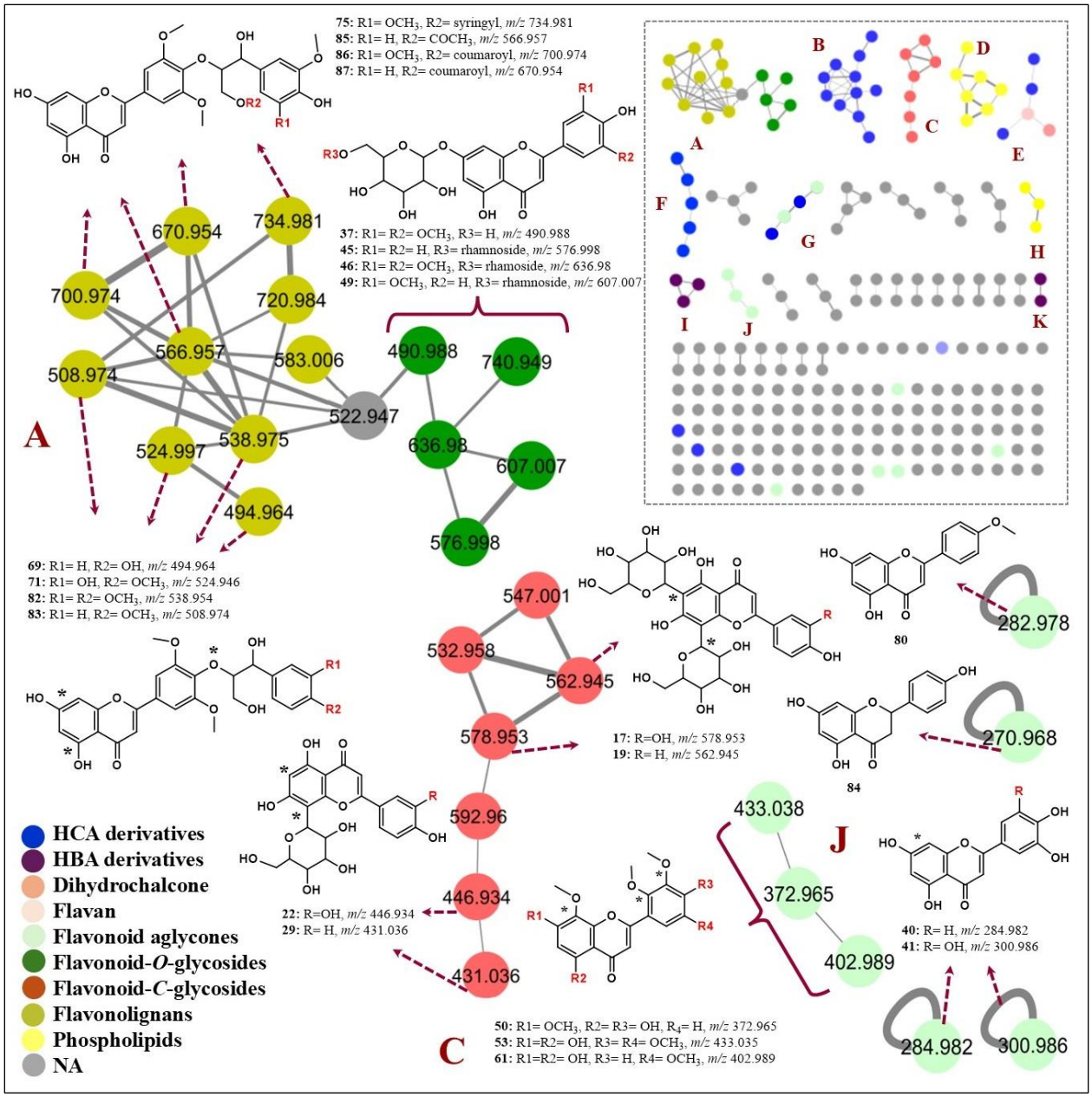

Figure 4. Molecular network of the negative LC-ESI-MS/MS spectra using the GNPS platform (upper left), showing enlarged clusters (**A**, **C**, and **J**) and self-looped nodes to illustrate different flavonoid sub-groups in *M. eruciformis*. Node colors represent different molecular families of the annotated metabolites.

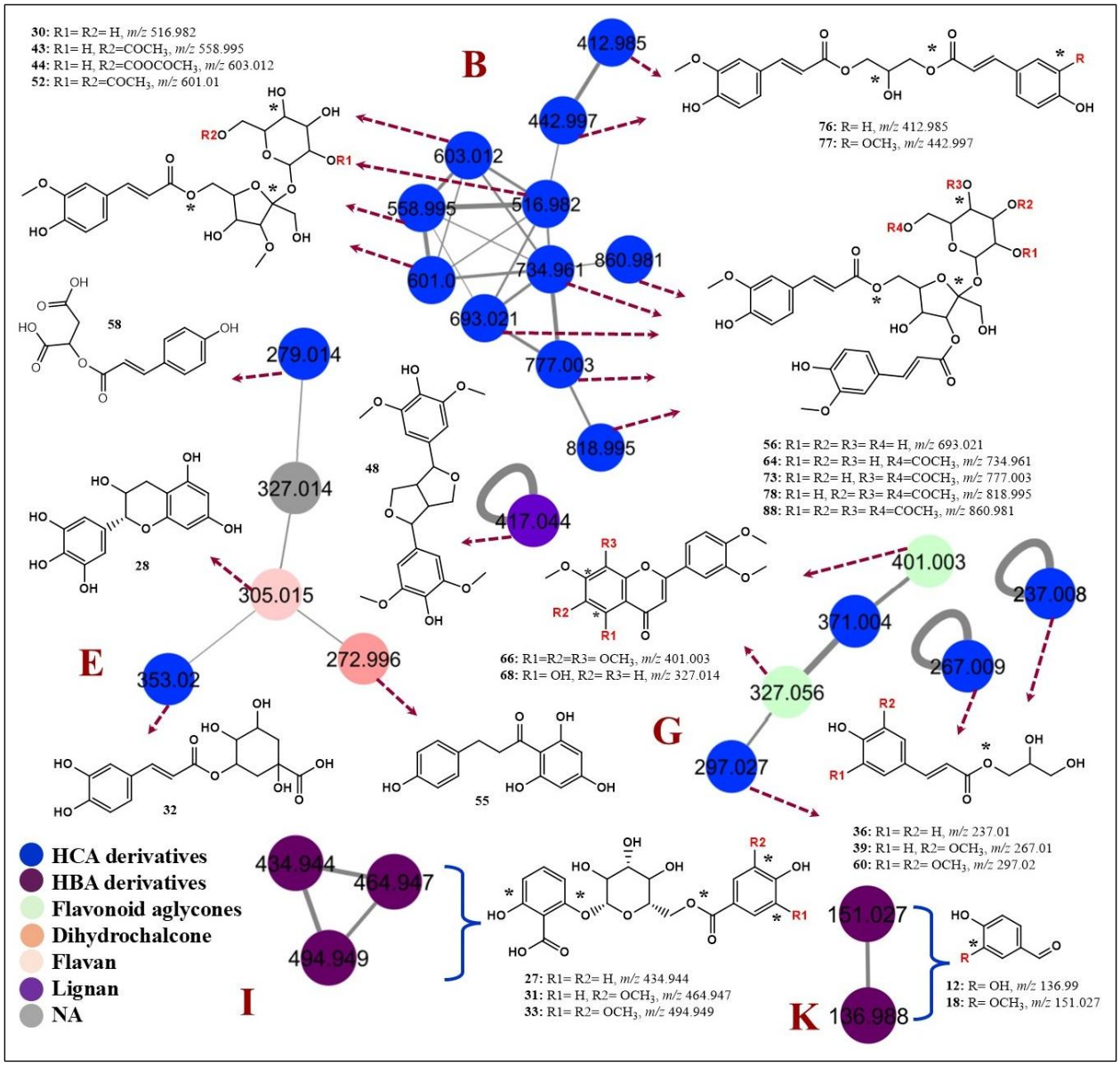

Figure 5. Clusters of interest (**B**, **E**, **G**, **I**, and **K**) illustrate examples of hydroxycinnamic acid derivatives (blue) and hydroxybenzoic acid derivatives (red) in *M. eruciformis*. Node colors represent different molecular families of the annotated metabolites.

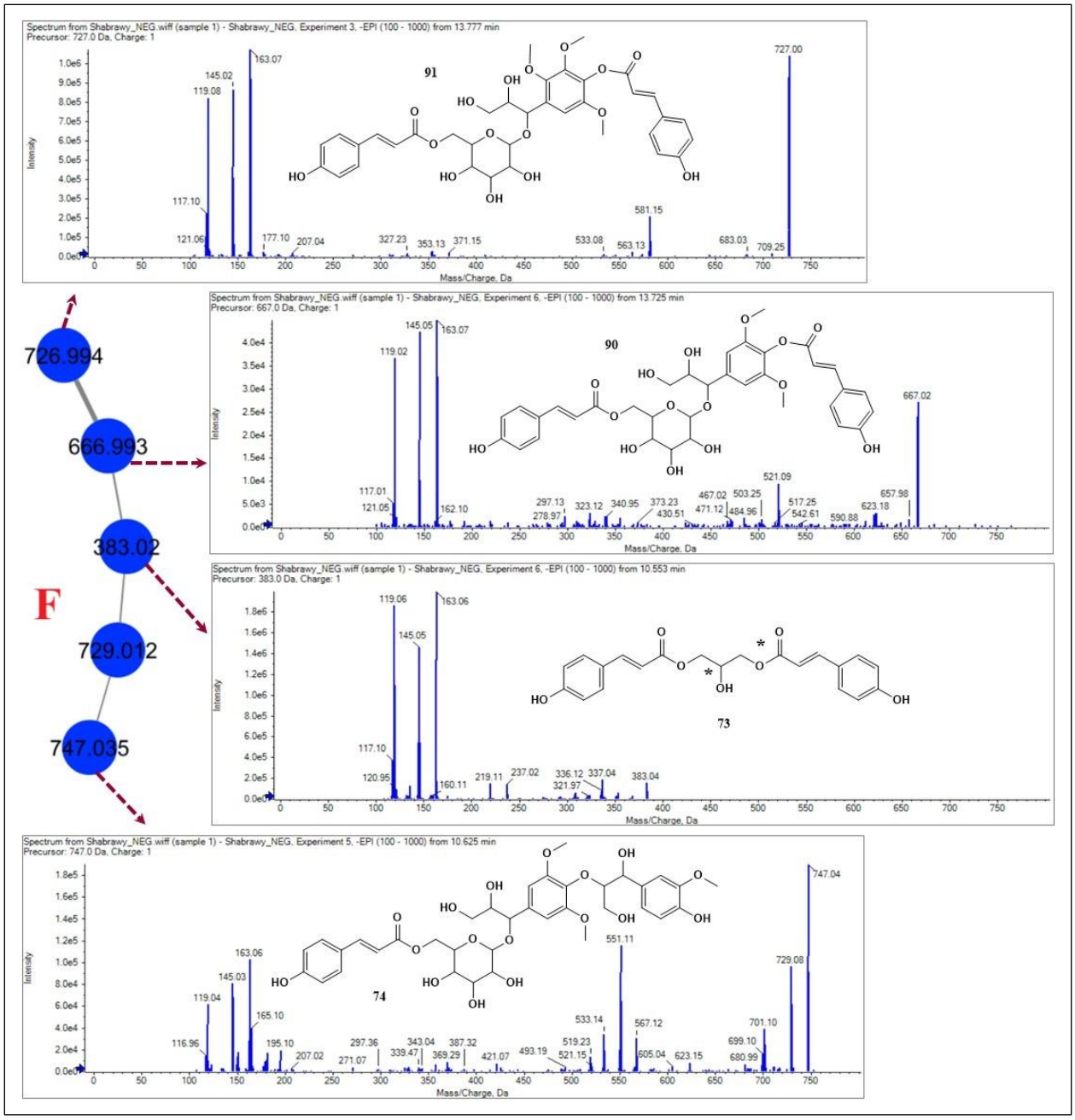

Figure 6. Cluster F illustrates some hydroxycinnamic acid structures in *M. eruciformis*, showing their MS spectra.

Table 1. Metabolites identified in the DAME of *M. eruciformis* by LC-ESI-MS/MS in negative ion mode

No.	Tentative identification	*Rt* (min)	$[M-H]^-$	Fragments	Ref.
Amino acids					
1	Threonine	0.33	117.97	100	[21]
3	Valine	0.94	116.08	99	[22]
8	Arginine	1.32	173.06	155, 137, 131, 113	[21]
11	Lysine	2.01	145.06	117	[21]
16	Tryptophan	2.31	203.08	175, 159, 157, 127	[22]
Organic acids					
2	Citric acid	0.91	191.01	111	[23]
4	Quinic acid	1.15	191.02	127, 111	[24]
Saccharides					
5	Disaccharide	1.21	341.11	179, 143, 119, 113, 101	[21]
Phenolic acids and derivatives					
	a. HCA and derivatives				
6	Caffeic acid [a]	1.24	179.12	163, 135	[25]
7	Sinapic acid [a,b]	1.31	223.02	163, 161, 149, 133, 119, 117	[26]
9	*p*-Coumaric acid [a,b]	1.35	163.02	135, 119	[25]
10	Feruloyl quinic acid [b]	1.68	366.993	193, 191, 173, 155, 137, 134, 111	[27]
13	Feruloyl quinic acid (isomer) [b]	2.11	366.993	193, 191, 173, 155, 137, 134, 111	[27]
14	*O*-Coumaric acid [a]	2.12	163.03	145, 135, 119	[25]
15	Dihydroferulic acid-O-glucuronide	2.19	371.004	249,195,175,121	[27]
20	Trihydroxy cinnamic acid	3.15	195.01	151, 150, 122, 108	[28]
26	Methoxy cinnamic acid	4.32	177.06	161, 133	[29]
30	Ferulic acid-*O*-dihexoside	4.69	516.98	337, 319, 265, 193, 179, 175, 160, 149, 133	[21]
32	Caffeoyl quinic acid	5.01	353.02	191, 179	[27]
36	Coumaroyl glycerol	5.64	237.01	163, 145, 119, 117	[30]
38	Ferulic acid [a]	6.05	193.08	179, 161, 149, 133	[24]
39	Feruloyl glycerol	6.31	267.01	252, 193, 179, 177, 160, 133, 105	[30]
43	Ferulic acid-*O*-acetyl dihexoside	6.7	558.995	517, 355, 193, 179, 175, 161, 149, 133	[31]
44	Ferulic acid-*O*-malonyl dihexoside	6.88	603.012	517, 355, 193, 179, 175, 161, 149, 133	[32]
52	Ferulic acid-*O*-diacetyl dihexoside	7.78	601.01	559, 517, 355, 193, 179, 175, 161, 149, 133	[32]
56	Ferulic acid-*O*-dihexoside ferulate (Helonioside A)	8.35	693.021	517, 499, 193, 179, 175, 161, 149, 133	[33]
58	Coumaroyl malate	8.47	279.01	163, 119	[15]
60	Sinapoyl glycerol	8.61	297.02	223, 206, 145	[30]
64	Ferulic acid-*O*-acetyl dihexoside ferulate (Helonioside B) = acetyl helonioside A	9.25	734.961	559, 541, 193, 179, 175, 161, 149, 133	[34]
72	Ferulic acid-*O*-diacetyl dihexoside ferulate (Smiglaside A) = diacetyl helonioside A	10.36	777.003	735, 601, 583, 559, 179, 175, 161, 149, 133	[32]
73	Dicoumaroyl glycerol	10.55	383.02	163, 145, 119	

74	Coumaric acid-*O*-guaiacylglyceryl-syringylglyceryl hexoside	10.63	747.035	551, 163, 145, 119	
76	Coumaroyl feruloyl glycerol	10.84	412.985	267, 193, 175, 163, 145, 134, 119	[30]
77	Diferuloyl glycerol	11.04	442.997	267, 207, 193, 175, 143	[35]
78	Ferulic acid-*O*-triacetyl dihexoside ferulate (Smiglaside C)	11.05	818.995	777, 759, 634, 601, 193, 175, 160, 134	[33]
88	Ferulic acid-*O*-tetraacetyl dihexoside ferulate (Acetyl smiglaside C)	12.21	860.981	819, 643, 587, 193, 175, 160, 134	[33]
90	Coumaric acid-*O*-coumaroyl guaiacylglyceryl hexoside	13.73	666.993	521, 163, 145, 119	
91	Coumaric acid-*O*-coumaroyl hydroxy trimethoxy phenyl glyceryl hexoside	13.78	726.994	581, 163, 145, 119	
	b. HBA and derivatives				
12	Dihydroxybenzaldehyde	2.07	136.988	121, 119, 108	
18	Hydroxy methoxy benzaldehyde/Vanillin	2.85	151.027	136, 124, 123, 109, 108	[25]
23	*p*-Hydroxy benzaldehyde [a,b]	3.61	121.01	108, 101	[25]
24	Hydroxy dimethoxy benzaldehyde/syringaldehyde	3.82	181.02	151, 121	[36]
25	Dimethoxybenzoic acid	4.11	181.02	167, 153, 137, 123, 107, 100	
27	Dihydroxybenzoic acid-*O*-(hydroxybenzoyl)-*O*-hexoside/ Parmentin	4.48	434.944	315, 153, 152, 137, 109	[37]
31	Dihydroxybenzoic acid-*O*-(hydroxy-methoxy benzoyl)-*O*-hexoside	4.78	464.947	435, 315, 167, 153, 109	[37]
33	Dihydroxybenzoic acid-*O*-(hydroxy-dimethoxy benzoyl)-*O*-hexoside	5.05	494.949	465, 315, 197, 183, 153, 109	[37]
35	Vanillic acid [a]	5.25	167.06	123, 108	[27]
Flavonoids					
	a. *C*-Glycosylflavonoids				
17	Luteolin 6-*C*-glucoside-8-*C*-arabinoside (Carlinoside)	2.67	578.953	561, 519, 489, 459, 441, 429, 399, 369	[38]
19	Apigenin 6-*C*-glucoside-8-*C*-arabinoside [b]	2.92	562.945	545, 503, 473, 443, 383, 353	[39]
21	Apigenin 6, 8-di-*C*-glucoside (Vicenin 2)	3.38	592.96	575, 503, 473, 383, 353	[38]
22	Orientin/isoorientin [b]	3.53	446.934	429, 357, 327, 297, 285	[23]
29	Vitexin/isovitexin	4.52	431.036	413, 341, 311, 283, 153	[40]
34	Apigenin 6,8-di-*C*-arabinoside [b]	5.21	532.958	515, 473, 443, 383, 353	
42	Apigenin 6-*C*-rhamnoside-8-*C*-arabinoside	6.52	547.001	529, 487, 473, 457, 443, 383, 353	[38]
	b. Flavonoid *O*-glycosides				
37	Tricin 7-*O*-glucoside [b]	5.93	490.988	329	[17]
45	Apigenin-7-*O*-rutinoside	7.18	576.99	530, 311, 269	[41]
46	Tricin-7-*O*-rutinoside [b]	7.34	636.98	329, 314, 299	
49	Diosmetin-7-*O*-rutinoside [b]	7.63	607.007	299, 284	[17]
89	Tricin acetyl di-glucoside [c]	12.25	740.949	695, 329, 314, 299	
	c. Flavonoid aglycones				
28	Gallocatechin	4.51	305.02	289, 275, 231, 203, 175, 147, 137	
40	Luteolin [a,b]	6.45	284.982	269, 267, 223, 205	[17]
41	Pentahydroxyflavone [b]	6.51	300.986	286, 285, 271, 269, 157, 243, 227	[23]

47	Tetrahydroxy-monomethoxyflavone	7.37	299.07	298, 283, 271, 253, 240	[23]
50	Dihydroxy-tetramethoxyflavone	7.73	372.965	359, 343, 329, 313, 299	[21]
53	Dihydroxy-hexamethoxyflavone	7.91	433.038	417, 402, 373, 358, 355	[23]
54	Dihydroluteolin (Eriodictyol)	7.98	287.18	269, 257, 241, 225	[23]
55	Phloretin	8.34	272.99	258, 243, 229, 215, 199,171, 167, 143	[23]
61	Dihydroxy-pentamethoxyflavone	8.73	402.989	357, 328, 327, 313, 285	[23]
65	Trihydroxy-trimethoxyflavone	9.46	359.09	313, 279, 253, 225	[23]
66	Hexamethoxyflavone	9.77	401.003	342, 325, 327, 312, 297	[23]
67	Tetrahydroxy-methoxy flavone	9.84	315.02	300, 271, 269, 193, 163	[23]
68	Hydroxy trimethoxy flavone	9.89	327.004	297, 282, 267, 253, 161, 109	[23]
70	Dihydroxy-dimethoxyflavone	10.01	313.07	299, 285, 251, 227	[23]
79	Tricin	11.13	329.02	314, 299, 283, 271	[17]
80	Acacetin [b]	11.16	282.98	268, 255, 163, 133, 117	[17]
81	Apigenin	11.28	268.99	253, 227, 117	[17]
84	Naringenin [b]	11.54	270.968	225, 197	[17]
	d. Flavonolignans				
45	Tricin 4`-*O*-hydroxy phenyl glycerol-7-*O*-glucoside	6.88	656.983	491, 329, 314	[42]
57	Tricin-*O*-guaiacyl glycerol-7-*O*-rutinoside	8.36	832.977	637, 329, 314, 299	[42]
59	Tricin 4`-*O*-guaiacyl glycerol-7-*O*-glucoside	8.53	686.97	525, 329, 314, 299	[42]
62	Tricin-O-di guaiacylglycerol	9.16	720.984	685, 673, 525, 329, 314, 299	[42]
63	Tricin-*O*-acetyl dihydroxy methoxy phenyl glycerol	9.21	583.006	535, 477, 329, 314, 299	[42]
69	Tricin-*O*-hydroxy phenyl glycerol	9.98	494.964	329, 314, 299, 165, 135	[42]
71	Tricin-*O*-hydroxy methoxy phenyl glycerol = Tricin-*O*-guaiacyl glycerol	10.14	524.997	329, 314, 299, 195, 165, 151, 123	[42]
75	Tricin-*O*-disyringyl glycerol	10.75	734.981	673, 555, 329, 299, 193, 175, 161, 149, 133, 119	[42]
82	Tricin-*O*-dimethoxy phenyl glycerol	11.32	538.975	477, 329, 314, 299	[43]
83	Tricin-*O*-methoxy phenyl glycerol	11.33	508.974	446, 329, 314, 299	[42]
85	Tricin -*O*-guaiacyl glycerol-*O*-acetate	11.61	566.957	329, 314, 299	[43]
86	Tricin-*O*-sryingyl glycerol-*O*-coumarate	11.72	700.974	555, 329, 314, 299	[43]
87	Tricin-*O*-guaiacylglycerol-*O*-coumarate	11.87	670.954	525, 329, 314, 163, 119	[43]
Lignan					
48	Syringaresinol	7.57	417.044	403, 387, 371, 193, 181, 166, 151, 137, 123, 109	[40]
Phospholipids					
92	Linoleoyl-glycero-phosphoinositol	13.99	595.096	415, 329, 315, 279, 241, 153	[21]
93	Hexadecanoyl-glycero-phosphoinositol [b]	14.52	571.101	391, 315, 271, 255, 241, 153	[21]
94	Hexadecanoyl-glycero-phosphoglycerol [b]	15.25	483.11	255, 245, 227, 171, 153	[21]
95	Octadecanoyl-glycero-phosphocholine [c]	16.39	564.123	518, 504, 279, 242, 224, 183, 153	[44]
96	Heptadecanoyl-glycero-phosphocholine	16.41	504.143	299, 279, 243, 224, 153	[44]

97	Hexadecanoyl-glycero-phosphocholine [c]	17.24	540.141	480, 255, 245, 224, 183, 153	[44]
98	Hexadecanoyl-glycero-phosphocholine isomer	17.25	480.18	404, 255, 224, 167	[44]
99	Octadecenoyl-glycero-phosphocholine [c]	17.82	566.141	506, 281, 242, 224, 153	[44]
100	Heptadecenoyl-glycero-phosphocholine [b]	17.96	506.159	281, 243, 224, 153	[44]
101	Eicosenoyl-glycero-phosphoinositol [c]	22.67	671.279	625, 445, 415, 391, 341, 279, 241, 153	[44]
102	Hydroxyoctadecenoyl-glycero-phosphoglycerol	22.89	525.332	297, 282, **271**, 253, 153	[44]

[a]; Standard, [b]; GNPS, [c]; $[M-H+FA]^-$

Phenolic acids and their derivatives

Phenolic acids are found frequently in various Poaceae species [45]. They are well known for their potential free radical scavenging activity, attributed to the phenolic hydroxyl groups present in their structures [46]. The position and presence of more hydroxyl groups on the aromatic ring, in conjunction with other substituents, can enhance their antioxidant properties. The antioxidative stress of phenolic acids can help protect against related diseases [47].

a. Hydroxycinnamic acids and derivatives

The identified phenolic acids in *M. eruciformis* are characterized by the predominance of the hydroxycinnamic acids and derivatives either in free (7 metabolites) or conjugated (23 metabolites) forms. The conjugated forms can be found as three esters of quinic acid, one malic acid ester, six esters of glycerol, and 13 glycosylated acids.

The generated characteristic fragmentation pattern of the free hydroxycinnamic acids [acid-H-H_2O]$^-$ and [acid-H-CO_2]$^-$ was synchronized with caffeic (**6**; *m/z* 179.12 $[M-H]^-$), sinapic (**7**; *m/z* 223.02 $[M-H]^-$), coumaric (**9 & 14**; *m/z* 163.02 $[M-H]^-$), ferulic (**38**; *m/z* 193.08 $[M-H]^-$), trihydroxy cinnamic (**20**; *m/z* 195.01 $[M-H]^-$), and methoxy cinnamic (**26**; *m/z* 177.06 $[M-H]^-$)

acids. They were previously reported as predominant compounds in various members of the Gramineae family but validated for the first time in our investigated species [45].

Besides free hydroxycinnamic acids, their ester forms of quinic acid, commonly known as chlorogenic acids, were annotated. The deprotonated molecular ions of the chlorogenic acids (**10**, **13**, **32**) participated in the fragment ion at *m/z* 191 of quinic acid and its key fragments (173 [M-H-H_2O]$^-$, 129 [M-H-H_2O-CO_2]$^-$, and 111 [M-H-2H_2O-CO_2]$^-$), in addition to the deprotonated fragment ion of each corresponding acid; such as *m/z* 193 for feruloyl quinic acid isomers (**10** and **13**; *m/z* 366.993 [M-H]$^-$) and *m/z* 179 for caffeoyl quinic acid (**32**; *m/z* 353.02 [M-H]$^-$). The lateral compound grouped in cluster **E** is associated with another hydroxycinnamic acid ester; coumaroyl malate (**58**; *m/z* 279.01 [M-H]$^-$), characterized by losing 116 Da, representing the malate moiety, and revealing diagnostic fragments at *m/z* 163 and 119, which correspond to coumaric acid (**Figure 5**).

Particularly, esterification of hydroxycinnamic acids with glycerol is also predominant in the members of the family Poaceae [30, 48]. The most predictable fragmentation signals for the annotation of the those phenylpropanoids in the investigated species are the fragments consistent with the specific deprotonated hydroxycinnamic acid anions; coumaroyl (*m/z* 163), feruloyl (*m/z* 193), sinapoyl (*m/z* 223) signified the elucidation of coumaryl glycerol (**36**; *m/z* 237.01 [M-H]$^-$), feruloyl glycerol (**39**; *m/z* 267.01 [M-H]$^-$), and sinapoyl glycerol (**60**; *m/z* 297.02 [M-H]$^-$), respectively. Sinapoyl glycerol was perceived in cluster **G** (**Figure 5**). In contrast, **36** and **39** nodes appeared isolated in MN as scattered self-looped nodes, reasonable by their fewer common fragments (2–5). This was insufficient in clustering, as the minimum requirement was six matched fragments. The predictable fragments of **73** (dicoumaroyl glycerol; *m/z* 383.02 [M-H]$^-$) were similar to three members of coumaric acid glycosides, resulting in its placement in cluster **F**

(**Figure 6**). The base peak of coumarate anion (*m/z* 163) guided the loss of coumaryl glycerol unit [M-H-237]$^-$. The other two HCAEs; coumaroyl feruloyl glycerol (**76;** *m/z* 412.985 [M-H]$^-$) and diferuloyl glycerol (**77**; *m/z* 442.997 [M-H]$^-$), are embedded nodes of cluster **B** (**Figure 5**). Their spectra gave rise to the intense ions of *m/z* 267 of feruloyl glycerol anion and *m/z* 193 assigned to the deprotonated ferulate ion, after loss of feruloyl (-176 Da) and coumaroyl (-146 Da) moieties, respectively.

Additionally, cluster **B** (**Figure 5**) correlated with nine other glycosylated compounds that shared the same diagnostic fragmentation pattern of ferulic acid (*m/z* 193, 179, 149, 133). Therefore, the parent ions of these compounds suggested ferulic acid derivatives with various hexosyl and acetyl units. Even though LC/MS/MS can putatively identify those compounds, the exact position of the acetyl group on the hexose moieties or differentiating the hexose isomers themselves cannot be proved without further analysis. Neutral loss of two hexose units [M-H-342]$^-$ justified ferulic acid-*O*-dihexoside (**30**; *m/z* 516.982 [M-H]$^-$) which directly connected to compounds **43**, **52**, and **44** in cluster **B** with a mass difference (42, 84, and 86 Da), confirming the additional (acetyl, diacetyl, and malonyl) groups, respectively, coincided with ferulic acid-*O*-acetyl dihexoside (**43**; *m/z* 558.995 [M-H]$^-$), ferulic acid-*O*-diacetyl dihexoside (**52**; *m/z* 601.01 [M-H]$^-$), and ferulic acid-*O*-malonyl dihexoside (**44**; *m/z* 603.012 [M-H]$^-$) (**Figure 5**). These four compounds also connected nodes **56**, **64**, **72**, **78**, and **88** in the same cluster, which share a core structure of diferulic acid glycosylated with two hexose units but differing in the degree of acetylation on those hexoses. The primary loss from ferulic acid-*O*-dihexoside ferulate (**56**; helonioside A, *m/z* 693.021 [M-H]$^-$) and ferulic acid-*O*-acetyl dihexoside ferulate (**64**; helonioside B, *m/z* 734.961 [M-H]$^-$) would be loss of the terminal feruloyl unit [M-H-176]$^-$ yielding daughter ions of *m/z* 517 and 559, then losing the dihexosyl and acetyl dihexosyl moieties, respectively, to

produce the ferulate anion. Conversely, as the remaining compounds contain more than one acetyl group (**72**, **78**, and **88**), the first to be lost could be one acetyl group, followed by the same manner; feruloyl unit, and then the mono-, di-, and tri-acetyl dihexosyl residuals. As the number of acetyl groups increases, the compound elutes later. Furthermore, the mass differences between them permitted their structures to be assumed. Ferulic acid-*O*-diacetyl dihexoside ferulate (**72**; smiglaside A, *m/z* 777.003 $[M-H]^-$), monitored by the daughter ions of 735 $[M-H\text{-acetyl}]^-$, 559 $[M-H\text{-acetyl-feruloyl}]^-$, 193 $[M-H\text{-acetyl-feruloyl-monoacetyl dihexosyl}]^-$. Ferulic acid-*O*-triacetyl dihexoside ferulate (**78**; smiglaside C, *m/z* 818.995 $[M-H]^-$) yielded product ions of 777 $[M-H-42]^-$, 601 $[M-H-(176+42)]^-$, 193 $[\text{Ferulic acid-H}]^-$. In another way, ferulic acid-*O*-tetra acetyl dihexoside ferulate (**88**; *m/z* 860.981 $[M-H]^-$) produced the fragments 819 $[M-H-42]^-$, 643 $[M-H-42-176]^-$, 193 $[\text{Ferulic acid-H}]^-$, after losing acetyl, acetyl feruloyl, then tetra acetyl dihexoside feruloyl yielding ferulic acid, respectively.

Furthermore, a monoglycosylated metabolite, dihydroferulic acid-*O*-glucuronide (**15**; *m/z* 371.004 $[M-H]^-$) lost a glucuronide sugar unit (176 Da) to exhibit *m/z* 195 for dihydroferulic acid ([33]).

A group of unique skeletons, considering the three complex coumaric acid glycosides (**74**, **90**, and **91**) clustered linked with dicoumaroyl glycerol (**73**) in cluster **F,** was tentatively identified for the first time in the grass family (**Figure 6**). Coumaric acid-*O*-guaiacylglyceryl-syringylglyceryl hexoside (**74**; *m/z* 747.035 $[M-H]^-$) missed the guaiacylglyceryl unit (*m/z* 551 $[M-H-196]^-$) and syringylglyceryl hexosyl (163 $[M-H-196-226-162]^-$), consequently. Coumaric acid-*O*-coumaroyl guaiacylglyceryl hexoside (**90**; *m/z* 666.993 $[M-H]^-$) and coumaric acid-*O*-coumaroyl hydroxy trimethoxy phenyl glyceryl hexoside (**91**; *m/z* 726.994 $[M-H]^-$) lost a coumaroyl moiety $[M-H-146]^-$ to produce intermediate fragments *m/z* 521 and 581, respectively.

Then, the prominent coumarate signal (*m/z* 163) quantified these molecules after losing guaiacylglyceryl hexosyl (196+162) and hydroxy trimethoxy phenyl glyceryl hexosyl (256+162) derivatives.

b. Hydroxybenzoic acids and derivatives

Nine hydroxybenzoic acid derivatives were represented in clusters **I**, **K**, and as self-looped nodes (**Figure 5**). Four benzaldehyde analogues out of the nine compounds are included in this group. They are designated as *p*-hydroxy benzaldehyde (**23**; *m/z* 121.01 $[M-H]^-$) and dihydroxybenzaldehyde (**12**; *m/z* 136.988 $[M-H]^-$), distinguished by losing the formyl radical (CHO). Vanillin (**18**; hydroxy methoxy benzaldehyde, *m/z* 151.027 $[M-H]^-$) and syringaldehyde (**24**; hydroxy dimethoxy benzaldehyde, *m/z* 181.02 $[M-H]^-$) were further illustrated by the characteristic loss of methyl groups. Compounds **12** and **18** shared six fragments to be collected in cluster **K**. The mass differences between the three specialized metabolites combined in cluster **I** draw attention to their annotation. Each compound is greater than the other by 30 Da, corresponding to an extra methoxyl group. Fragmentation pattern pointed out dihydroxybenzoic acid hexoside linked to hexose sugar, and further connected to hydroxybenzoic acid isomers, first reported in the family Poaceae. Expecting fragments of dihydroxybenzoic acid hexoside at *m/z* 315 for all, hydroxybenzoic acid hexoside at *m/z* 299 (**27**), hydroxy methoxybenzoic acid hexoside at *m/z* 329 (**31**), and hydroxy dimethoxybenzoic acid hexoside at *m/z* 359 (**33**), allowed the identification of these complex molecules; dihydroxybenzoic acid-*O*-(hydroxybenzoyl)-*O*-hexoside (**27**; Parmentin, *m/z* 434.944 $[M-H]^-$), dihydroxybenzoic acid-*O*-(hydroxy-methoxy benzoyl)-*O*-hexoside (**31**; *m/z* 464.947 $[M-H]^-$), and dihydroxybenzoic acid-*O*-(hydroxy-dimethoxy benzoyl)-*O*-hexoside (**33**; *m/z* 494.949 $[M-H]^-$). Vanillic acid (**35**; hydroxy methoxy benzoic acid, *m/z* 167.06 $[M-H]^-$) was nominated by the *m/z* 123 daughter ion due to

decarboxylation, while dimethoxybenzoic acid (**25**; *m/z* 181.02 $[M-H]^-$) was nominated by the subsequent loss of the methyl groups.

Flavonoids

Diverse profiles of flavonoids across the crop's family, rice, wheat, maize, sorghum, foxtail millet, and broomcorn millet, vary between flavones, flavanones, and anthocyanin contents [10]. They displayed potent bioactivities and are linked to many health benefits. The flavonoids of *M. eruciformis* are distinguished as *C*-glycosylflavonoids (7), flavonoid *O*-glycosides (5), flavonoid aglycones (18), and flavonolignans (13), but not previously reported for the species.

a. C-Glycosylflavonoids

The constructed cluster **C** gathers seven *C*-glycosyl flavone conjugates, identified for the first time in the considered species (**Figure 4**). Their peaks eluted earlier in the first half of the base peak chromatogram (R_t 2.67 - 6.52). They shared a peak of $[M-H-18]^-$ due to loss of water, followed by sugar cross-ring cleavages exhibiting peaks of $[M-H-60/90]^-$ for *C*-pentosides, $[M-H-90/120]^-$ for *C*-hexosides, and $[M-H-104/74]^-$ for *C*-deoxyhexosides. On the other hand, the sugar remains that are still attached to the aglycone determine the degree of glycosylation, whether mono *C*-glycoside (aglycone + 41/71) or di *C*-glycoside (aglycone + 83/113). For *M. eruciformis*, mono-*C*-glucosyl luteolin was synchronized with compound **22** (orientin; *m/z* 446.9 $[M-H]^-$) while apigenin isomer was corroborated with **29** (vitexin) by *m*/z 431.1 $[M-H]^-$ participating ions at *m/z* 311 $[270 + 41]^-$ and 341 $[270 + 71]^-$. Its glycosylation position was inferred from the higher abundance of product ion *m/z* 311 $[M-H-120]^-$ [49]. Conversely, apigenin di-*C*-symmetric glycoside derivatives; apigenin 6, 8-di-*C*-glucoside (**21**; *m/z* 593 $[M-H]^-$) and apigenin 6,8-di-*C*-arabinoside (**34**; *m/z* 532.9 $[M-H]^-$) in addition to apigenin di-*C*-asymmetric glycoside; apigenin

6-*C*-glucoside-8-*C*-arabinoside (**19**; *m/z* 562.9 $[M-H]^-$) and apigenin 6-*C*-rhamnoside-8-*C*-arabinoside (**42**; *m/z* 547 $[M-H]^-$) shared fragments at *m/z* 353 $[270 + 83]^-$ and 383 [270 + 113]. Their mass spectrum differentiated the type and position of both linked sugars. The higher abundance of the sugar cleavage fragments of each indicates its attachment at the 6-position. Compound **19** signalized *m/z* 443 $[M-120]^-$ much more abundant than *m/z* 503 $[M-60]^-$ proposing 6-*C*-glucosyl unit in addition to *m/z* 473 $[(M-H)-90]^-$ base peak. Likewise, compound **42** showed more intense fragments of rhamnosyl moiety 473 $[M-74]^-$ and 443 $[M-104]^-$ relative to arabinose [28]. Moreover, luteolin 6-*C*-glucoside-8-*C*-arabinoside was typically established (**17**; *m/z* 578.9 $[M-H]^-$) [38]. These compounds were isolated beforehand from other grass species [50-52].

b. Flavonoid O-glycosides

Cluster **A** began linking closely interrelated mono- and di-*O*-glycosyl flavones, as well as flavonolignans (**Figure 4**), and GNPS determined their structures. Monosaccharide flavone was identified in peak **37** as tricin 7-*O*-glucoside (*m/z* 490.988 $[M-H]^-$), which is widely recognized earlier in the family Poaceae [35, 53]. Nodes **45**, **49**, and **46** were closely associated, derived from the loss of the rutinoside moiety $[M-H-308]^-$ tentatively assigned as apigenin 7-*O*-rutinoside *m/z* 576.998 $[M-H]^-$, diosmetin 7-*O*-rutinoside *m/z* 607.007 $[M-H]^-$, and tricin 7-*O*-rutinoside *m/z* 636.98 $[M-H]^-$, respectively. Compound (**89**) was noticed as a formic acid adduct ion at *m/z* 740.949 $[M-H+FA]^-$ and the abundant ion at *m/z* 329 $[M-H-162-162-42-46]^-$, suggesting tricin acetyl diglucoside structure.

c. Flavonoid aglycones

The diagnostic key ions of peaks **40, 79, 80**, and **81** annotated flavone aglycones; luteolin (*m/z* 284.982), tricin (*m/z* 329.02), acacetin (*m/z* 282.98), and apigenin (*m/z* 268.99), respectively.

Nevertheless, flavanone aglycones were illustrated as dihydroluteolin (**54**; Eriodictyol, *m/z* 287.18 [M-H]$^-$) and naringenin (**84**; *m/z* 270.968 [M-H]$^-$). Moreover, pentahydroxyflavone (**41;** *m/z* 300.986) and nine polyhydroxy polymethoxylated flavones aglycones (**47**, **50**, **53**, **61**, **65**, **67**, **68**, **70**) continued to produce intermediate fragment ions through the loss of water, carbon monoxide, and repeated loss of a methyl radical (-CH2, -14 Da). Both **66** and **68** were gathered in cluster **G** (Figure 4)**,** while **50**, **53**, and **61** were determined in cluster **J** (Figure 4). A flavan-3-ol skeleton aglycone **28** (gallocatechin; *m/z* 305.02 [M-H]$^-$) and a dihydrochalcone structure **55** (phloretin; *m/z* 272.99 [M-H]$^-$) were gathered in cluster **E** (**Figure 5**). These aglycones have not been reported previously in *M. eruciformis.*

d. Flavonolignans

The polyphenolic compounds are formed by the combination of a flavonoid moiety (tricin, often found in grasses) [41] with a phenylpropanoid unit (lignan; frequently phenyl glycerol in Poaceae) [35]. Their structural diversity arises from the aromatic ring of phenyl glycerol, starting from hydroxyphenyl glycerol (184 Da), methoxyphenyl glycerol (198 Da), hydroxy methoxy glycerol (guaiacyl glycerol, 214 Da), dimethoxy glycerol (228 Da), and ending with hydroxy dimethoxy glycerol (syringyl glycerol, 244 Da). These metabolites are of particular interest because they have unique biological and chemical characteristics that can vary from those of their parent flavonoids and lignans, and have not yet been documented in our species.

In *M. eruciformis*, flavonolignans were identified as a prominent group, comprising 11 compounds in cluster A and two other self-looped nodes representing the glycosides, which were documented for the first time in this species (**Figure 4**). They were all flavonolignan derivatives of tricin on the basis that their mass spectra showed a diagnostic major product ion at *m/z* 329

[tricin-H]$^-$. The precursor ions at *m/z* 494.964 [329 + 166]$^-$, *m/z* 508.974 [329 + 180]$^-$, *m/z* 524.997 [329 + 196]$^-$, and *m/z* 538.975 [329 + 210]$^-$ corresponded to tricin-*O*-hydroxy phenyl glycerol (**69**), tricin-*O*-methoxy phenyl glycerol (**83**), tricin-*O*-hydroxy methoxy phenyl (guaiacyl) glycerol (**71**), and tricin-*O*-dimethoxy phenyl glycerol (**82**), respectively. In addition, compound (**71**) is directly attached to compound (**85**) through a mass difference of 42 Da as a probable acetyl group (*m/z* 566.957 [M-H]$^-$; tricin-*O*-guaiacyl glycerol-*O*-acetate), which in turn linked to another acetyl derivative **63**; with a mass shift of 16 Da for an extra hydroxyl moiety (*m/z* 583.006 [M-H]$^-$). Another thick edge connecting the nodes of coumaroyl congeners coincide with tricin-*O*-guaiacyl glycerol-*O*-coumarate (**87**; *m/z* 670.954 [M-H]$^-$) and tricin-*O*-syringyl glycerol-*O*-coumarate (**86**; *m/z* 700.974 [M-H]$^-$). Tricin-*O*-di guaiacyl glycerol (**62**; *m/z* 720.984 [M-H]$^-$) exhibited daughter ions at *m/z* 525 [M-H-196]$^-$ and *m/z* 329 [M-H-196-196]$^-$ after subsequent loss of guaiacyl glycerol units. It was seen linked to tricin-*O*-disyringyl glycerol (**75**; *m/z* 734.981 [M-H]$^-$) with mass difference (14 Da), which gives a fragment at *m/z* 555 [M-H-180]$^-$, missing one syringyl group, then the syringyl glycerol moiety exhibited a *m/z* 329 [M-H-180-226]$^-$ fragment. The self-looped flavonolignan glycosides could be differentiated through molecular ions at *m/z* 656.983 [M-H]$^-$ (tricin 4'-*O*-hydroxy phenyl glycerol-7-*O*-glucoside) and product ion at *m/z* 491.04 [M-H-162]$^-$ for **45**, [M-H]$^-$ at *m/z* 686.97 (tricin -*O*-guaiacyl glycerol-*O*-glucoside) and product ion at *m/z* 525 [M-H-162]$^-$ for **59**, and [M-H]$^-$ at *m/z* 832.977 (tricin-*O*-guaiacyl glycerol-*O*-rutinoside) with fragment ion at *m/z* 637.01 [M-H-196]$^-$ followed by loss of rutinoside moiety [M-H-196-308]$^-$ confirming peak **57**.

Lignan

To a lesser extent, syringaresinol (**48**; *m/z* 417.044 [M-H]$^-$) is an identified lignan by the fragments reported by [54]. The fragment at *m/z* 403 corresponded to the loss of a methyl radical

(-14 Da), while *m/z* 387 (-30 Da) and 371 (-15 Da) represented the neutral loss of a formaldehyde molecule, followed by a methyl group. It can be found in various cereals [55]; nonetheless, it was first found in the investigated plant.

Phospholipids

The structural relationships between different phospholipid classes were visualized in clusters **D** and **H (Figure 4)**, particularly phosphatidylinositol, phosphatidylglycerol, and phosphatidylcholine (Table 1). Until now, it's the first report on phospholipid constituents in *M. eruciformis.* The characteristic fragment ion at *m/z* 241 is characterize to identify linoleoyl-glycero-phosphoinositol (**92**; *m/z* 595.096 $[M-H]^-$), hexadecanoyl-glycero-phosphoinositol (**93**; *m/z* 571.101 $[M-H]^-$), eicosenoyl-glycero-phosphoinositol (**101**; *m/z* 671.279 $[M-H+FA]^-$), as well as the product ions *m/z* 415, 391 $[M-H-180]^-$, and 445 $[M-H-46-180]^-$, indicating inositol moiety loss, respectively. Hexadecanoyl-glycero-phosphoglycerol (**94**; *m/z* 483.11 $[M-H]^-$) and hydroxyoctadecenoyl-glycero-phosphoglycerol (**102**; *m/z* 525.332 $[M-H]^-$) were described through a mono-dehydrated glycerophosphate unit (*m/z* 153) and glycerophosphoglycerol unit (*m/z* 245). **93** and **94** were confirmed through GNPS.

Most phosphocholine class compounds in negative ionization mode are detected as adducts with formate anions $[M-H+46]^-$. After losing the adduct anion, these compounds lost a methyl group from the choline moiety $[M-H-46-14]^-$. Furthermore, the product ion at *m/z* 183 marked those molecules. Octadecanoyl-glycero-phosphocholine (**95**; *m/z* 564.123 $[M-H+46]^-$), and hexadecanoyl-glycero-phosphocholine (**97**; *m/z* 540.141 $[M-H+46]^-$), octadecenoyl-glycero-phosphocholine (**99**; *m/z* 566.141 $[M-H+46]^-$) coexisted as formic acid adducts. The product ions of 504, 480, and 506 were generated by losing a CH_3 group after CH_2O_2 anions. Heptadecanoyl-glycero-phosphocholine (**96**; *m/z* 504.143 $[M-H]^-$), hexadecanoyl-glycero-phosphocholine isomer

493 (**98**; *m/z* 480.18 $[M-H]^-$), and heptadecanoyl-glycero-phosphocholine (**100**; *m/z* 506.159 $[M-H]^-$)
494 were marked.
495
496 **Discussion**
497 The most environmentally friendly, safest, and sustainable alternative to synthetic
498 pharmaceuticals is medicinal plants, which have a wide range of potential therapeutic uses. Plants
499 synthesize a vast array of secondary metabolites that act synergistically through various
500 mechanisms of action on multiple targets and pathways. Plant-derived compounds possess
501 multifunctional bioactive properties, particularly antioxidant and anti-inflammatory abilities,
502 which provide health benefits in alleviating chronic diseases involving oxidative stress and
503 inflammation. Scavenging harmful free radicals and modulating inflammatory signaling pathways
504 are interconnected with the induction and progression of chronic conditions, such as
505 neurodegenerative diseases and type 2 diabetes mellitus. The significant correlation between the
506 total phenolic content and the antioxidant capabilities, as well as inhibition of metabolic enzymes,
507 indicated that the phenolics are the major contributors to these properties. Their unique structures
508 allow them to work together, with those sharing similar active features potentially playing parallel,
509 complementary, or even overlapping roles in conceivable activities [56].

510 The antioxidant capacity of phenolic acids and aldehydes enables them to interact directly
511 with free radicals through single-electron or hydrogen-atom transfer, or to trigger the expression
512 of endogenous antioxidant enzymes. Furthermore, they can alter signaling pathways involved in
513 inflammation, such as those involving NF-κB, inhibit the synthesis of pro-inflammatory cytokines,
514 suppress cyclooxygenase enzymes, and modify the expression of certain receptors, including

GLUT-2, thereby enhancing insulin signaling. Methyl and ethyl esters exhibited a higher inhibition of acetylcholinesterase than their respective free acids [57, 58, 59].

Hydroxybenzoic acid derivatives showed promise as therapeutic agents for oxidative stress-related inflammatory diseases. 2,4-Dihydroxybenzoic acid (*β*-resorcylic acid) and 3,4-dihydroxybenzoic acid (protocatechuic acid) scavenged the free radicals directly, upregulated the antioxidant enzymes, and protected against lipid peroxidation. *β*-Resorcylic acid anti-neuroinflammatory effects were by reducing chemokines and altering microglial phenotypes, while protocatechuic acid inhibited NF-κB and MAPK pathways, reduced pro-inflammatory mediators like TNF-α and IL-1β, and interfered with leukocyte recruitment [57]. Protocatechuic acid inhibited α-glucosidase, decreasing mice's postprandial blood glucose levels [60]. Vanillic acid (4-hydroxy-3-methoxybenzoic acid) ameliorated scopolamine-induced learning and memory impairment in rats by modulating acetylcholine esterase activity and oxidative stress [61], inhibited α-glucosidase and α-amylase enzymes involved in starch digestion and proteases from snake venom [62, 63].

The antioxidant and anti-inflammatory activities of vanillin (4-hydroxy-3-methoxybenzaldehyde) were demonstrated through scavenging hydrogen peroxide and reactive oxygen species, preventing lipid peroxidation, maintaining antioxidant enzymes activity, while reducing pro-inflammatory cytokine expression in activated macrophages [64, 65]. Syringaldehyde (hydroxy dimethoxy benzaldehyde) reduced glucose absorption in diabetic mice by inhibiting α-amylase and increasing intestinal motility [66] and interacted with acetylcholine esterase in a docking study by [67]. 4-Hydroxybenzaldehyde also showed potent acetylcholine esterase inhibition [68].

Regarding the hydroxy cinnamic acids and their derivatives, the pharmacological potential of phenolic acids as coumaric, caffeic, ferulic, sinapic, and chlorogenic acids was verified to have antioxidant and anti-inflammatory activities relevant to Alzheimer's and diabetes management. Research on their effect on proteinases is less common. Caffeic acid showed superior inhibitory effects compared to chlorogenic acid against α-glucosidase, α-amylase, and acetylcholine esterase [69]. The antioxidant potency of caffeic acid > ferulic acid > coumaric acid > chlorogenic acid through free radical scavenging and metal chelation. Esterification of caffeic acid with quinic acid reduced the activity [70, 71]. Sinapic acid proved to exhibit impacts such as neuroprotective through inhibiting cholinesterase enzyme, antioxidant by enzyme enhancement, anti-inflammatory via T-helper 2 immune response suppression, in addition to anticancer bioactivities [72].

Diverse beneficial chemical and pharmacological characteristics of flavonoids depend on the structure class skeletons as the double bond between C2-C3, 4-carbonyl group, location and number of the hydroxyl groups at 3, 5, 7-positions of A, C rings and 3′, 4′, and 5′ of ring B, modification by methylation, acylation, and *O*-/*C*-glycosylation (amounts, types, position) mediate their effects [73]. Aglycones are generally considered more bioavailable than glycosides as they are more easily absorbed, metabolized, and distributed. However, some flavonoid glycosides showed superior *in vivo* abilities due to their slower absorption and metabolism and thus showed long-lasting effects. Glycosides can enhance the chemical stability of the compounds, increase water solubility, decrease toxicity, and improve a drug's specific targeting characteristic. Furthermore, glycosylation prevents plant molecules from autooxidation. Generally, *O*-glycosylation appeared to decrease the compounds' bioavailability, noted for anti-inflammatory, antioxidant, and antidiabetic activities. Anti-cholinesterase decreased by 1-5 times depending on the sugar moiety and the conjunction site. On the other hand, *O*-glycosylation can improve some

other bioactivities. Broad generalizations regarding the effect of glycosylation on the benefits of flavonoids are not achievable due to a lack of *in vivo* investigations. Glycosylation bioactivity of flavonoid *in vitro* might not be the same as that observed *in vivo*. Compared to their flavonoid aglycones, the glycosides demonstrated comparable or even greater antidiabetic, anti-inflammatory, and antiallergic efficacy when administered orally *in vivo. C*-glycosides are more resistant to hydrolysis due to the covalent bond between the sugar and aglycone, appear to have higher antioxidant and antidiabetic health outcomes than their corresponding aglycones or *O*-glycosides. Flavonoid *C*-monoglycosides are poorly absorbed and deglycosylated and broken down by human intestinal bacteria in the colon, but flavonoid *C*-multiglycosides are absorbed unaltered in the intestine and transported to various tissues (74, 52, 75, 76].

The antioxidant capacity of flavonoid aglycones and glycosides, as well as their ability to inhibit enzymes involved in carbohydrate metabolism, are frequently reported. Apigenin, acacetin, luteolin, tricin, naringenin, and eriodictyol scavenge the free radicals, chelate metals, inhibit oxidant enzymes, reduce oxidative stress, and prevent ROS-induced damage [77, 78, 79, 80; 81, 82]. Remarkable anti-inflammatory effect, potentially preventing complications of diabetes and neurodegenerative diseases, was recorded as α-glucosidase, α-amylase, and anticholinesterase inhibitors for apigenin [83; 84, 26], luteolin [85,86], naringenin [87,88], and eriodictyol (89, 90]. With respect to flavonoid glycosides, they provided the antioxidant benefits throughout tricin derivatives. Tricin 7-*O*-(6"-methoxycinnamic)-glucoside effect against DPPH was higher than Trolox [91]. Tricin 7-*O*-glucoside showed neuroprotective properties, reducing apoptosis in neuronal cells and providing cerebral ischemia protection through inhibition of NF-κB activation and HMGB1 expression [92]. Apigenin-7-O-glucopyranoside was identified as a potent α-

582 glucosidase inhibitor (IC50 = 22.80 μM) [93] and demonstrated strong *in vitro* antioxidant effects
583 and significant inhibition of acetylcholinesterase [94].

584 Regarding *C*-glycosyl flavonoids, vitexin/isovitexin reduced the intracellular reactive
585 oxygen species, noting that vitexin is more effective as a nitric oxide scavenger, while isovitexin
586 efficiently scavenges superoxide radicals. As anti-inflammatory agents, they inhibited
587 proinflammatory mediators such as IL-1β, IL-6, IL-8, IL-17, IL-33, TNF-α, and COX-2, and
588 enhanced the anti-inflammatory IL-10. Orally, they inhibited α-glucosidase and α-amylase.
589 Isovitexin was most potent acetylcholine esterase inhibitor than vitexin [95]. The antioxidant
590 properties of isoorientin are much higher than those of orientin [96]. Orientin reduced
591 inflammatory mediators as TNF-α, IL-6, NF-κB, and ERK1/2 [97] and showed a promising α-
592 glucosidase inhibitory effect through molecular docking and molecular dynamics studies [98].
593 Vicenin 2 revealed significant antioxidant and anti-diabetic activities via strong inhibition of α-
594 glucosidase, as well as suppression of glycation-induced protein oxidation [99]. Ogidigo et al.
595 (2021) [100] established potent antioxidant activity (IC_{50} = 7.382 ± 0.79 μg/mL for DPPH radical
596 scavenging) and significant anticholinesterase activity (IC_{50} = 22.283 ± 0.27 μg/mL) for
597 carlinoside.

598 A wide range of specific biological activities was recorded for flavonolignans, such as
599 antioxidant, anti-inflammatory, antidiabetic, vasodilator, and antiaging properties which may
600 benefit Alzheimer's disease [101]. Flavonolignans inhibited proteases such as leukocyte elastase
601 and gelatinases, which are implicated in inflammation. Specific structural features, like galloyl or
602 hydroxyl groups, are crucial for this activity [102]. Tricin 4'-*O*-(threo-β-guaiacylglyceryl) ether
603 and its threo isomer inhibited LPS-induced nitric oxide and reactive oxygen species generation by
604 down-regulating iNOS and COX-2 expression through NF-κB and STAT3 pathways. Both

isomers showed superior effect compared to tricin alone, and the erythro form showed the strongest one [103]. They showed > 65% anti-inflammatory effect in carrageenan-induced rat paw edema [104].

Identifying the relationships between structure and activity requires suitable techniques to understand how synergy functions. The use of metabolomics and molecular networking is very helpful for elucidating structures and modeling how compounds interact. Understanding the synergy of metabolites guides the development of metabolic and neurological applications, making valuable products out of invasive plant waste.

Conclusion

Focusing on discovering new analogues by the present study, *M. eruciformis,* a natural weed of the rice crop family *Poaceae*, can be used as a possible source of valuable products, encouraging environmentally friendly weed management techniques. The three extracts of *M. eruciformis* whole plant; petroleum ether, 70% aqueous methanol, and defatted aqueous methanol, were screened *in vitro* for antioxidant, anti-inflammatory, anti-Alzheimer, and antidiabetic properties. The effective defatted aqueous methanol was further analyzed using LC-ESI-MS. The complexity of the fractions is visually represented by MN, which can enhance understanding of the chemical nature of its metabolites, illustrate the concept of their relations, or simply enrich their structure elucidation. Furthermore, computational tools play a vital role in discovering potential drug candidates, as the similarity of the identified compounds to known bioactive compounds aids in identifying potential drug candidates. Nearly 102 compounds were tentatively annotated first in the studied species, 83 of which were chiefly phenolics. Several promising and interesting structures, including acetyl ferulic acid *O*-hexoside derivatives, coumaric acid-*O*-

coumaroyl hexoside conjugated with different phenyl glycerol unit, and flavonolignans were tentatively elucidated. They could be responsible for metabolic and neurological impacts. In combination with other compounds, these compounds are multi-target inhibitors for treating Alzheimer's disease and diabetes by targeting acetylcholinesterase, proteinase, α-glucosidase, and α-amylase enzymes, taking into consideration that their effects on bioactivity *in vitro* might not be the same as those observed *in vivo.* Further combined analysis is required to fully identify these structures. *M. eruciformis* whole plant Although they show promise as therapeutic agents for oxidative-stress-related inflammatory disease, additional data regarding their impact on bioactivity *in vivo* is required. *M. eruciformis* displays a diverse range of bioactivity, but it is yet to be established as a viable therapeutic candidate for more *in vivo* assessment and clinical experiments.

References

1. Damor, K., Kadia, R. and Modi, N. A review of phytochemical and pharmacological analysis of *Poaceae* family plants. *Int. J. Sci. Res. Sci. Technol.* **12**(1), 450-462 (2025).
2. Shavanov, M.V. The role of food crops within the *Poaceae* and *Fabaceae* families as nutritional plants. In *IOP Conference Series: Earth Environ. Sci.* **624**(1), 012111). IOP Publishing (2021).
3. Rojas-Sandoval, J., Meléndez-Ackerman, E. J., & Anglés-Alcázar, D. Assessing the impact of grass invasion on the population dynamics of a threatened Caribbean dry forest cactus. *Biol. Conserv.* **196**, 156-164 (2016).
4. Sagar, A. & Sarwar, A.G. Weed diversity of the family *Poaceae* in Bangladesh Agricultural University campus and their ethnobotanical uses: *Poaceae* grasses in BAU and their uses. *J. Bangladesh Agric. Univ.* **16**(3), 372-379 (2018).
5. Hussain A. Ecological utilisation of the weeds. *Int. J. Res. Publ. Rev.* **5**(6), 4654-4657 (2024).
6. Bilanda, D. C. et al. Antihypertensive activity of *Leersia hexandra* Sw. (Poaceae) aqueous extract on ethanol-induced hypertension in wistar rat. *Evid. Based Complement. Alternat. Med.* **2019**(1), 2897867 (2019).
7. Swargiary, A., Daimari, M., & Roy, M. K. Putative anthelmintic plants used in traditional medicine system of Kokrajhar district, India. *Ethnobot. Res. Appl.* **22**, 10 (2021).
8. Edem, U. A., Udobang, J. A., Bassey, A. L., Iyanyi, U. L., & Okokon, J. E. Antiulcerogenic activity of leaf extract of *Saccharum officinarum* (*Poaceae*) in rodents. *Niger. J. Pharm. Appl. Sci. Res.,* **12**(2), 22-27 (2023).
9. Andriamalala, S. G. et al. Diuretic activity of ethanolic extract of imperata cylindrical (l.) P. Beauv. (poaceae) leaves on rat. **14**(2), 719-724 (2023).
10. Tang, J. et al. Differential flavonoids and carotenoids profiles in grains of six *Poaceae* crops. *Foods*. **11**(14), 2068 (2022).

11. Vorontsova, M. S. Revision of some Malagasy forage grasses and their relatives within *Brachiaria, Echinochloa, Moorochloa,* and *Urochloa. Candollea*. **77**(2),199-236 (2022).
12. Boulos, L. Flora of Egypt, (Monocotyledoneae: Alismataceae–Orchidaceae), **4** (Al-Hadara Publishing: Cairo, Egypt, 2005).
13. Salgotra, R. & Chauhan, B. S. The First Report of target-site resistance to glyphosate in sweet summer grass (*Moorochloa eruciformis*). *Plants* **10**, 1885 (2021)
14. Ayeni, P. O. et al. Phytochemical analysis of *Brachiaria* grasses from Bowen University dairy farm and molecular docking of constituents with insulin-like growth factor binding protein. *Inform. Med. Unlocked*, **43**, 101386 (2023).
15. Farid, M. M. et al. Metabolomic profiling and DNA-fingerprinting of newly recorded white-flowered populations of *Salvia lanigera* Poir. in Egypt. *Chem. Biodiversity*. **21**(6), e202400619. (2024).
16. Farid, M. M., Aboulthana, W. M., Sayed, S. S. & Sokkar, N. M. Micropropagation of *Euphorbia milii* Des Moul. with bioguided preliminary phytochemical studies of its bioactive constituents. *S. Afr. J. Bot.*, **179**, 234-245 (2025).
17. Marzouk, M. M. et al. Isoflavone-rich extract of *Trifolium resupinatum*: anti-obesity attributes with in silico investigation of its constituents. *Rev. Bras. Farmacogn.* **34**(3), 522-535 (2024).
18. Hegazi, N. M. et al. UPLC-HRMS/MS Guided Isolation and NMR Investigation of Major Flavonoids from *Enarthrocarpus strangulatus* Boissier (*Brassicaceae*) with *In Vitro* Enzymes Inhibitory Potential. *Chem. Biodiversity.*, **22**, e202401402 (2024**).**
19. Aboulthana, W. M. et al. Phyto-and biochemical study on cape gooseberry (Physalis peruviana L.) extract incorporated with metal nanoparticles against hepatic injury induced in rats. *Nat. Prod. Res.*1-14 (2024).
20. Wang, M. et al. Sharing and community curation of mass spectrometry data with global natural products social molecular networking. *Nat. Biotechnol*. **34**(8), 828-837 (2016).
21. Marzouk, M. M. et al. Discriminative metabolomics analysis and cytotoxic evaluation of flowers, leaves, and roots extracts of *Matthiola longipetala* subsp. *livida. Metabolites*. **13**(8):909 (2023).
22. El Shabrawy, M. O. et al. Phytochemical profiling, cytotoxic effect, and *In Vitro* anti-diabetic assessment of *Asparagus horridus* L. with *In Silico* insights of brassicin. *Egypt. J. Chem.* **68**(12), 583–600 (2025).
23. Ragheb, A.Y. et al. MS/MS-based molecular networking for mapping the chemical diversity of the pulp and peel extracts from *Citrus japonica* Thunb.; in vivo evaluation of their anti-inflammatory and anti-ulcer potential. *Sci. Afr.* **20**, e01672 (2023).
24. Salem, M. A. et al. Spectrometric analysis, chemical constituents and cytotoxic evaluation of *Astragalus sieberi* DC. (*Fabaceae*). *Sci. Afr.* **7**, e00221 (2020).
25. Hegazi, et al. N. M. Molecular networking leveraging the secondary metabolomes space of *Halophila stipulaceae* (Forsk.) Aschers. and *Thalassia hemprichii* (Ehrenb. ex Solms) Asch. in tandem with their chemosystematics and antidiabetic potentials. *Mar drugs*, **19**, 279 (2021).
26. Zhou, X., Wang, F., Zhou, R., Song, X. & Xie, M. Apigenin: A current review on its beneficial biological activities. J. *Food Biochem*. **41**(4), e12376 (2017).
27. Farias, C. A. A. et al. Phenolic diversity and antioxidant potential of different varieties of bamboo leaves using LC-ESI-QTOF-MS/MS and LC-ESI-QqQ-MS/MS. *Food Res. Int.* **179**, 114025 (2024).
28. Farag, M. A. et al. Comparative metabolite fingerprinting of four different Cinnamon species analyzed via UPLC-MS and GC-MS and chemometric tools. *Molecules*. 27, 2935 (2022).

29. Wang, P. et al. Identification of differential compositions of aqueous extracts of *Cinnamomi ramulus* and *Cinnamomi cortex*. *Molecules*. **28**(5), 2015 (2023).
30. Varga, M., Jójárt, R., Fónad, P., Mihály, R. & Palágyi, A. Phenolic composition and antioxidant activity of colored oats. *Food Chem.*, **268**, 153-161 (2018).
31. Nosrati Gazafroudi, K., Mailänder, L. K., Daniels, R., Kammerer, D. R. and Stintzing, F. C., From Stem to spectrum: Phytochemical characterization of five Equisetum species and evaluation of their antioxidant potential. *Molecules*, **29**(12), 2821 (2024).
32. Yue, C. et al. Qualitative analysis of chemical constituents and study on the biological activity of Polygonum perfoliatum L. *Nat. Prod. Res.* 1-9 (2024).
33. Gegentana, Xu. F. et al. 20 potentially new compounds and 11 new bioactive constituents found in Smilacis Glabrae Rhizoma utilizing HPLC-DAD-ESI-IT-TOF-MSn. *Phytochem. Anal.* **35**(5), 1186-1196 (2024).
34. Sweilam, S. H., Abd El Hafeez, M. S., Mansour, M. A. & Mekky, R. H. Unravelling the phytochemical composition and antioxidant potential of different parts of *Rumex vesicarius* L.: A RP-HPLC-MS-MS/MS, chemometrics, and molecular Docking-Based comparative study. *Plants*, **13**(13), 1815 (2024).
35. Yang, Z. et al. Toward better annotation in plant metabolomics: isolation and structure elucidation of 36 specialized metabolites from *Oryza sativa* (rice) by using MS/MS and NMR analyses. *Metabolomics*. **10**, 543–555 (2014).
36. Gomes August, E. M. et al. Seasonal phenolic profile, antioxidant, and photoprotective activities of *Psidium guajava* L. leaves. *Chemistry & Biodiversity*. **22**(5), e202402852 (2025).
37. Rahmani Samani, M. et al. Phytochemical investigation and biofilm-inhibitory activity of *Bachtiari savory* (*Satureja bachtiarica* Bunge) aerial parts. *Plants*, **13**(1), 67 (2023).
38. Marzouk, M. M. et al. *C*-glycosyl flavonoids-rich extract of *Dipcadi erythraeum* Webb & Berthel. bulbs: Phytochemical and anticancer evaluations. *J. Appl. Pharm. Sci.* **9**(6), 094-098 (2019).
39. Ragheb, A.Y. et al. Comparative Chemical Investigation of *Brachychiton australis* (Schott & Endl.) A. Terracc. and *Brachychiton discolor* F. Muell. *Egypt. J. Chem.* **64**(10), 5529-5536 (2021).
40. Lin, Y. et al. Phytochemical compositions and biological activities of the branches and leaves of *Ormosia hosiei* Hemsl. et Wils. *J. Pharm. Biomed. Anal.*, **226**, 115238 (2023).
41. Marzouk, M. M. et al. Comparative study of *Mentha* species growing wild in Egypt: LC-ESI-MS analysis and chemosystematic significance. *J. Appl. Pharm. Sci*, **8**(8), 116-122 (2018).
42. Lan, W. et al. Tricin-lignins: occurrence and quantitation of tricin in relation to phylogeny. Plant J. **88**(6), 1046-57 (2016).
43. Lan, W. et al. Maize tricin-oligolignol metabolites and their implications for monocot lignification. *Plant Physiol*. **171**(2), 810-820 (2016).
44. Pulfer, M. & Murphy., R. C. Electrospray mass spectrometry of phospholipids. Mass Spectrom. Rev., **22**(5), 332–364 (2003).
45. Favaretto, A., Scheffer-Basso, S. M. & Perez, N. B. Allelopathy in *Poaceae* species present in Brazil. A review. *Agron. Sustainable Dev*. **38**(2), 22 (2018).
46. Platzer, Melanie, et al. Radical scavenging mechanisms of phenolic compounds: A quantitative structure-property relationship (QSPR) study. *Front. Nutr.* **9**, 882458 (2022).
47. Kumar, N., Goel, N. Phenolic acids: Natural versatile molecules with promising therapeutic applications. Biotechnology reports. **24**, e00370 (2019).

48. Aly, O. et al. Deciphering the potential of *Cymbopogon citratus* (DC.) Stapf as an anti-obesity agent: Phytochemical profiling, in vivo evaluations and molecular docking studies. *Food Funct.* **15**(24), 2146-68 (2024).
49. Ferreres, F., Silva, B. M., Andrade, P. B., Seabra, R. M. & Ferreira, M. A. Approach to the study of *C*-glycosyl flavones by ion trap HPLC-PAD-ESI/MS/MS: application to seeds of quince (*Cydonia oblonga*). Phytochemical Analysis. *Int. J. Plant Chem. Biochem. Tech.* **14**(6), 352-359 (2003).
50. Figueirinha, A., Paranhos, A., Pérez-Alonso, J. J., Santos-Buelga, C. & Batista, M. T. *Cymbopogon citratus* leaves: Characterization of flavonoids by HPLC–PDA–ESI/MS/MS and an approach to their potential as a source of bioactive polyphenols. *Food Chem*. **110**(3), 718-728. (2008).
51. Rauter, A. P., Lopes, R. G. & Martins, A. *C*-Glycosylflavonoids: Identification, bioactivity and synthesis. *Nat. Prod. Commun*. 2(11), 1934578X0700201125 (2007).
52. Xiao, J., Capanoglu, E., Jassbi & A. R., Miron A. Advance on the flavonoid *C*-glycosides and health benefits. *Crit. Rev. Food Sci. Nutr*. **56**(sup1), S29-45 (2016).
53. Mauricio Duarte-Almeida, J. et al. Antiproliferative and antioxidant activities of a tricin acylated glycoside from sugarcane (*Saccharum officinarum*) juice. Phytochemistry. **68**(8), 1165-1171 (2007).
54. Zamljen, T., Slatnar, A., Hudina, M., Veberic, R. & Medic, A. Characterization and quantification of capsaicinoids and phenolic compounds in two types of chili olive oils, using HPLC/MS. *Foods*. **11**(15), 2256 (2022).
55. Zhang, L. et al. A comprehensive review on the plant sources, pharmacological activities and pharmacokinetic characteristics of syringaresinol. *Pharmacol. Res.* **212**, 107572 (2025).
56. Leyane, T. S., Jere, S. W. & Houreld, N. N. Oxidative stress in ageing and chronic degenerative pathologies: molecular mechanisms involved in counteracting oxidative stress and chronic inflammation. *Int. J. Mol. Sci.* **23**(13), 7273 (2022).
57. López-Herrador, S. Natural hydroxybenzoic and hydroxycinnamic acids derivatives: mechanisms of action and therapeutic applications. *Antioxidants*. **14**(6), 711 (2025).
58. Borgohain, R., Guha, A. K., Pratihar, S., Handique, J. G. Antioxidant activity of some phenolic aldehydes and their diimine derivatives: A DFT study. *Comput. Theor. Chem.***1060**,17-23 (2015).
59. Szwajgier, D. Anticholinesterase activity of phenolic acids and their derivatives. *Z. Naturforsch. C.* **68**(3-4), 125-132 (2013).
60. Ding, H. et al. Blood glucose-lowering activity of protocatechuic acid is mediated by inhibiting α-glucosidase. *Food Sci. Hum. Wellness*. **13**(3), 1212-1219 (2024).
61. Choi, G. Y. et al. Ameliorative effect of vanillic acid against scopolamine-induced learning and memory impairment in rat via attenuation of oxidative stress and dysfunctional synaptic plasticity. Biomedicine & Pharmacotherapy. **177**, 117000 (2024).
62. Cai, R., et al. Extraction, partial purification and characterisation of vanillic acid decarboxylase from *Alicyclobacillus acidoterrestris* DSM 3923. *J. Sci. Food Agric*. **96**(8), 2925-2931 (2016).
63. Aleixandre, A., Gil, J. V., Sineiro, J., Rosell, C. M. Understanding phenolic acids inhibition of α-amylase and α-glucosidase and influence of reaction conditions. *Food Chem*. **372**, 131231 (2022).
64. Kwon, J. et al. Inflammation-responsive antioxidant nanoparticles based on a polymeric prodrug of vanillin. *Biomacromolecules*. **14**(5), 1618-26 (2013).

65. Makni, M. et al. Evaluation of the antioxidant, anti-inflammatory and hepatoprotective properties of vanillin in carbon tetrachloride-treated rats. *Eur. J. Pharmacol.* **668**(1-2), 133-139 (2011).
66. Weng, L. et al. Syringaldehyde promoting intestinal motility with suppressing α-amylase hinders starch digestion in diabetic mice. *Biomed. Pharmacother*. **141**, 111865 (2021).
67. Wu, J. et al. A narrative review: The pharmaceutical evolution of phenolic syringaldehyde. *Biomed. Pharmacother.* **153**, 113339 (2022).
68. Yu, L. et al. Design, synthesis and evaluation of difunctionalized 4-hydroxybenzaldehyde derivatives as novel cholinesterase inhibitors. *Chem. Pharm. Bull*. **58**(9), 1216-1220 (2010).
69. Oboh, G., Agunloye, O. M., Adefegha, S. A., Akinyemi, A. J. & Ademiluyi, A. O. Caffeic and chlorogenic acids inhibit key enzymes linked to type 2 diabetes (in vitro): a comparative study. J. *Basic Clin. Physiol. Pharmacol*. **26**(2), 165-170 (2015).
70. Damasceno, S. S., Dantas, B. B., Ribeiro-Filho, J., Antônio M. Araújo, D., Galberto M. da Costa, J. Chemical properties of caffeic and ferulic acids in biological system: implications in cancer therapy. A review. *Curr. Pharm. Des*. **23**(20), 3015-3023 (2017).
71. Sørensen, A. D. et al. Antioxidant properties and efficacies of synthesized alkyl caffeates, ferulates, and coumarates. *J. Agric. Food Chem*. **62**(52), 12553-12562 (2014).
72. Nićiforović, N. & Abramovič, H. Sinapic acid and its derivatives: natural sources and bioactivity. *Compr. Rev. Food Sci. Food Saf*. **13**(1), 34-51 (2014).
73. Hossain, M. K. et al. Molecular mechanisms of the anti-obesity and anti-diabetic properties of flavonoids. *Int. J. Mol. Sci*.**17**(4), 569 (2016).
74. Xie, Y., Yang, W., Chen, X., & Xiao, J. Inhibition of flavonoids on acetylcholine esterase: binding and structure–activity relationship. *Food Funct.* **5**(10), 2582-2589 (2014).
75. Xiao J. Dietary flavonoid aglycones and their glycosides: Which show better biological significance?. *Crit. Rev. Food Sci. Nutr*. **57**(9), 1874-1905 (2017).
76. Xie, L. et al. Comparison of flavonoid *O*-glycoside, *C*-glycoside and their aglycones on antioxidant capacity and metabolism during in vitro digestion and in vivo. *Foods.* **11**(6), 882 (2022).
77. Al-Badri, S. R. & Al-Janabi, N. M. Effect of temperature and ph on the antioxidant activity of tricin flavonoid extracted from Rice bran. IOP Conference Series: *Earth Environ. Sci.* IOP Publishing. **1225**(1), 012060 (2023).
78. Kashyap, P., Shikha, D., Thakur, M. & Aneja, A. Functionality of apigenin as a potent antioxidant with emphasis on bioavailability, metabolism, action mechanism and in vitro and in vivo studies: A review. *J. Food Biochem.* **46**(4), e13950 (2022).
79. Mahwish, I. M. et al. Antioxidative and anticancer potential of Luteolin: a comprehensive approach against wide range of human malignancies. *Food Sci. Nutr*. **13**(1), e4682 (2025).
80. Yao, L. et al. A comprehensive review of pharmacological and analytical aspects of acacetin. (2021).
81. Uçar, K. & Göktaş, Z. Biological activities of naringenin: A narrative review based on in vitro and in vivo studies. *Nutr. Res.* **119**, 43-55 (2023).
82. Jing, X. et al. Eriodictyol attenuates β-amyloid 25–35 peptide-induced oxidative cell death in primary cultured neurons by activation of Nrf2. *Neurochem. Res*. **40**(7),1463-71 (2015).
83. Cichon, N. et al. Mechanistic and Therapeutic insights into flavonoid-based inhibition of acetylcholinesterase: implications for neurodegenerative diseases. *Nutrients*. **17**(1), 78 (2024).
84. Zeng, L., Zhang, G., Lin, S. & Gong, D. Inhibitory mechanism of apigenin on α-glucosidase and synergy analysis of flavonoids. *J. Agric. Food Chem*. **64**(37), 6939-6949 (2016).

85. Choi, J. S. et al. The effects of *C*-glycosylation of luteolin on its antioxidant, anti-Alzheimer's disease, anti-diabetic, and anti-inflammatory activities. *Arch. Pharmacal Res.* **37**(10),1354-63 (2014).
86. Tadera, K., Minami, Y., Takamatsu, K. & Matsuoka, T. Inhibition of α-glucosidase and α-amylase by flavonoids. *J. Nutr. Sci. Vitaminol.* **52**(2), 149-153 (2006).
87. Heo, H. J. et al. Naringenin from *Citrus junos* has an inhibitory effect on acetylcholinesterase and a mitigating effect on amnesia. *Dementia Geriatr. Cognit. Disord*. **17**(3), 151-157 (2004).
88. Priscilla, D. H., Roy, D., Suresh, A., Kumar, V. & Thirumurugan, K. Naringenin inhibits α-glucosidase activity: A promising strategy for the regulation of postprandial hyperglycemia in high fat diet fed streptozotocin induced diabetic rats. *Chem.-Biol. Interact*. **210**, 77-785 (2014).
89. He, P. et al. Eriodictyol attenuates LPS-induced neuroinflammation, amyloidogenesis, and cognitive impairments via the inhibition of NF-κB in male C57BL/6J mice and BV2 microglial cells. *J. Agric. Food Chem*. **66**(39), 10205-10214 (2018).
90. Lim, J., Zhang, X., Ferruzzi, M. G., Hamaker, B. R. Starch digested product analysis by HPAEC reveals structural specificity of flavonoids in the inhibition of mammalian α-amylase and α-glucosidases. *Food Chem*. **288**, 413-421 (2019).
91. Duarte-Almeida J. M., Negri, G., Salatino, A., de Carvalho, J. E. & Lajolo, F. M. Antiproliferative and antioxidant activities of a tricin acylated glycoside from sugarcane (*Saccharum officinarum*) juice. *Phytochemistry*. **68**(8), 1165-1171 (2007).
92. Jiang, W. L., Xu, Y., Zhang, S. P., Zhu, H. B. & Hou, J. Tricin 7-glucoside protects against experimental cerebral ischemia by reduction of NF-κB and HMGB1 expression. *Eur. J. Pharm. Sci*. **45**(1-2), 50-57 (2012).
93. Jia, Y., Ma, Y., Cheng, G., Zhang Y & Cai, S. Comparative study of dietary flavonoids with different structures as α-glucosidase inhibitors and insulin sensitizers. *J. Agric. Food Chem*. **67**(37), 10521-10533 (2019).
94. Costa Marques, T. H. et al. Phytochemical profile and qualification of biological activity of an isolated fraction of *Bellis perennis*. *Biol. Res*. **46**(3), 231-238 (2013).
95. He, M. et al. A review on the pharmacological effects of vitexin and isovitexin. *Fitoterapia*. **115**, 74-85 (2016).
96. Li, Y., Yu-chen, W. U., Xiao-meng, R. E. N., Xue-bo, L. I. U. Comparison of antioxidant activities and cytotoxicity in hepG2 cells of orientin and isoorientin. *J. Food Sci. Technol*. **31**, 21–7 (2014).
97. Lee, W., Ku, S. K. & Bae, J. S. Vascular barrier protective effects of orientin and isoorientin in LPS-induced inflammation in vitro and in vivo. *Vasc. Pharmacol.* **62**(1), 3-14 (2014).
98. Sadeghi. M., Shakouri Khomartash, M. & Taslimi, P. The potential of *C*-Glycosylflavonoids as α-glucosidase inhibitors determined by virtual screening, molecular docking, molecular dynamics, and IC_{50} studies. *ChemistrySelect*. **8**(20), e202300847 (2023).
99. Islam, M. N., Ishita, I. J., Jung, H. A. & Choi, J. S. Vicenin 2 isolated from *Artemisia capillaris* exhibited potent anti-glycation properties. Food Chem. Toxicol. **69**, 55-62 (2014).
100. Ogidigo, J. O. et al. UPLC-PDA-ESI-QTOF-MS/MS fingerprint of purified flavonoid enriched fraction of *Bryophyllum pinnatum*; antioxidant properties, anticholinesterase activity and in silico studies. *Pharm. Biol.* **59**(1), 442-454 (2021).
101. Křen, V. Chirality Matters: Biological activity of optically pure silybin and its congeners. *Int. J. Mol. Sci.* **22**(15), 7885 (2021).

102. Sartor, L. et al. Inhibition of matrix-proteases by polyphenols: chemical insights for anti-inflammatory and anti-invasion drug design. *Biochem. Pharmacol.* **64**(2), 229-37 (2002).
103. Jung, Y. S. et al. Anti-inflammatory effect of tricin 4′-O-(threo-β-guaiacylglyceryl) ether, a novel flavonolignan compound isolated from Njavara on in RAW264. 7 cells and in ear mice edema. *Toxicol. Appl. Pharmacol*. **277**(1), 67-76 (2014).
104. Mohanlal, S., Parvathy, R., Shalini, V., Helen, A. & Jayalekshmy, A. Isolation, characterization and quantification of tricin and flavonolignans in the medicinal rice Njavara (*Oryza sativa* L.), as compared to staple varieties. *Plant Foods Hum. Nutr*. **66**(1), 91-96 (2011).

Acknowledgment

The authors thank the National Research Centre, Giza, Egypt, for providing the resources for this study.

Authors contributions

Alia Y. Ragheb: conceptuality; data curation; methodology (extraction and fractionation); writing the original draft; reviewing; and editing. **Mona El Shabrawy**: investigation; visualization; experimental (extraction and fractionation); and writing the original draft. **Amal G. Hussien**: conceptuality; biological assays; validation; and draft reviewing and editing. **Mona E. S. Kassem** conceptualization, suggesting and collecting the plant; supervision; writing; and reviewing. **Mona M. Marzouk**: conceptualization; formal analysis; resources; software; LC-ESI-MS analyses; structure elucidation; writing the original draft; reviewing; and editing. The published manuscript has been read, edited, and approved by all the writers.

Funding

The plant collection and extraction procedures were funded by the National Research Centre, Cairo, Egypt (Project number 11010328).

Competing interests

The authors declare no competing interests.

Consent for publication

We further confirm that the content has not been published or submitted for publication elsewhere.

Data Availability Statement:

The molecular network, parameters, and MS spectra can be accessed via the link: https://gnps.ucsd.edu/ProteoSAFe/status.jsp?task=4d581a781b434fa18c9298e3d8e292d1, created on August 7, 2024.

Correspondence and requests for materials should be addressed to M. O.-EL & M. M.-M.